NASA Technical Memorandum 107750

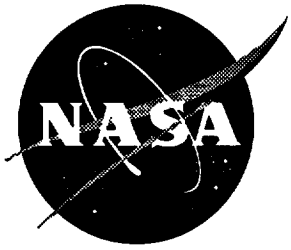

A Structural Design Decomposition Method Utilizing Substructuring

Stephen J. Scotti
Langley Research Center, Hampton, Virginia

January 1994

National Aeronautics and
Space Administration
Langley Research Center
Hampton, Virginia 23681-0001

A STRUCTURAL DESIGN DECOMPOSITION METHOD UTILIZING SUBSTRUCTURING

Stephen J. Scotti
NASA Langley Research Center
Hampton, Virginia

Abstract

The present paper describes a new method of design decomposition for structural analysis and optimization. For this method, the structure is divided into substructures where each substructure has its structural response described by a structural-response subproblem, and its structural sizing determined from a structural-sizing subproblem. The structural responses of substructures that have rigid body modes when separated from the remainder of the structure are further decomposed into displacements that have no rigid body components, and a set of rigid body modes. The structural-response subproblems are linked together through forces determined within a structural-sizing coordination subproblem which also determines the magnitude of any rigid body displacements. Structural-sizing subproblems having constraints local to the substructures are linked together through penalty terms that are determined by a structural-sizing coordination subproblem. All the substructure structural-response subproblems are totally decoupled from each other, as are all the substructure structural-sizing subproblems, resulting in the significant potential for use of parallel solution methods for these subproblems.

Introduction

Nonlinear mathematical programming (NLP) is extensively used for optimal structural sizing in structural design. The most computationally efficient NLP methods at present incorporate approximation concepts, such as developed in reference 1, that require both the structural response of the entire structure and the response sensitivity derivatives with respect to all the design variables. These approximation-based NLP structural-sizing methods have been very successful and are implemented in several commercial structural analysis codes.

Further improvements in the computational efficiency of NLP structural-design methods are desired, especially for the detail design of structures requiring a large number of design variables and constraints. One approach to the solution of large problems is to decompose a large problem into a set of smaller subproblems. If most of the smaller subproblems can be solved separately and in parallel, the time required to find the optimum design can be significantly reduced. By repeating this decomposition process at the subproblem level, a multilevel decomposition (ref. 2 and references therein) can be obtained. One concern in the decomposition of an optimum design problem is whether any solution exists to the decomposed problem. If a solution exists, another concern is whether this solution to the decomposed problem is also a solution to the original problem. The present paper addresses these concerns, and develops a formal method for solving structural-design problems which are decomposed using substructuring.

Specifically, derivations are presented for a decomposition of the minimum weight design process when each design constraint depends only on the design variables and structural response of a single substructure. Stress and local buckling constraints and certain displacement constraints fall into this category of design constraint. For this decomposition method, the structure is partitioned into substructures in a manner that allows for solution of the structural response and the structural optimization on a substructure-by-substructure basis. The present decomposition method also has several unique aspects that allow for efficient computation, much of which can be done in parallel. The theory of the decomposition method is discussed utilizing a two-substructure example and the derivation for an arbitrary number of substructures is presented in the appendix.

Theory

The method of determining the structural response of a structure that is decomposed into substructures is presented first. This response solution method is then utilized in formulating a set of Equilibrium Programming (EP) subproblems that determine the optimal design. The derivation which follows demonstrates the method using two substructures which are assumed to have a linear elastic response. The appendix summarizes the method for an arbitrary number of substructures.

Decomposition of the Structural Response

The present structural-response decomposition method has some similarity to the work presented in reference 3 in that the present method is a substructuring approach which utilizes Lagrange multipliers to enforce compatible displacements at the interfaces between substructures. Four salient features characterize the present method. The structural response of each substructure is decomposed into the rigid body motions (referred to as "modes" herein) of the substructure, and displacements that have strain energy but no rigid body motion. Secondly, an augmented stiffness

matrix is formed for each substructure. These stiffness matrices are symmetric, and can be factored independently and, computationally, in parallel. Thirdly, a structural-response coordination problem determines the internal forces between the substructures (i.e., the Lagrange multipliers), and the rigid body modes. The structural-response coordination problem requires the factored, augmented stiffness matrices of the substructures, and results in a system of linear equations with the number of degrees-of-freedom equal to the number of shared degrees-of-freedom between substructures plus the total number of substructure rigid body modes. Lastly, once the internal forces between the substructures are determined, the displacements having strain energy can be determined.

The simple wing structure finite element model in figure 1 is utilized to demonstrate the derivation of the present decomposition method. The model shown in the figure is decomposed into two substructures, the second of which has rigid body modes. Only one loading condition is considered in the derivation; however, the derivation is easily extended to multiple loading conditions. The displacements of the entire wing for a given loading condition are denoted by the nodal displacement vector $\mathbf{U}$, and the displacements of the two substructures are given by the vectors $\mathbf{U}_1$ and $\mathbf{U}_2$. The displacements at the interface of the two substructures must be equal for the two substructures to be compatible. Those displacements at the interfaces of the two substructures that must be compatible are chosen in a predetermined order with signed Boolean matrices denoted by $\mathbf{B}_1$ and $\mathbf{B}_2$, where the nonzero entries of $\mathbf{B}_1$ are equal to $+1$ and the nonzero entries of $\mathbf{B}_2$ are equal to -1. The constraints of compatible displacements at the interface between substructures is then expressed by $\mathbf{B}_1\mathbf{U}_1 + \mathbf{B}_2\mathbf{U}_2 = \mathbf{0}$. The external loading for the entire wing is given by the nodal force vector $\mathbf{F}$, and the decomposition of the external loading is given by vectors $\mathbf{F}_1$ and $\mathbf{F}_2$ for the two substructures. The decomposition of the externally applied nodal forces at the interface nodes is arbitrary as long as the sum of the forces applied to the interface nodes of each substructure is equal to the actual externally applied forces.

The linear elastic structural response for the entire wing is determined using a minimum potential energy formulation. This response is the solution to the unconstrained minimization problem given by

$$\min_{\mathbf{U}} \left(\frac{1}{2}\mathbf{U}^T\mathbf{K}\mathbf{U} - \mathbf{F}^T\mathbf{U} \right) \tag{1}$$

where the first term is the strain energy of the structure, and the second term is the work done by the external forces. The necessary conditions for the unconstrained minimization problem represented by statement (1) simplify to the linear equations:

$$\mathbf{K}\mathbf{U} = \mathbf{F} \tag{2}$$

where $\mathbf{K}$ is the global stiffness matrix. In a substructural decomposition, a stiffness matrix can be formulated for each substructure. These stiffness matrices are relative to the substructure nodal displacement vectors $\mathbf{U}_i$, and are denoted by $\mathbf{K}_i$. Thus a constrained minimization problem that is equivalent to the problem given by statement (1) and uses the substructure nodal displacement vectors is

$$\begin{aligned} \min_{(\mathbf{U}_1,\mathbf{U}_2)} & \left(\frac{1}{2}\mathbf{U}_1^T\mathbf{K}_1\mathbf{U}_1 + \frac{1}{2}\mathbf{U}_2^T\mathbf{K}_2\mathbf{U}_2 \right. \\ & \left. -\mathbf{F}_1^T\mathbf{U}_1 - \mathbf{F}_2^T\mathbf{U}_2 \right) \\ & \mathbf{B}_1\mathbf{U}_1 + \mathbf{B}_2\mathbf{U}_2 = \mathbf{0} \end{aligned} \tag{3}$$

At first glance, the constrained minimization problem given by statement (3) appears to be separable, i.e., the problem can be decomposed into two distinct minimization problems, with design variables $\mathbf{U}_1$ and $\mathbf{U}_2$, respectively, and a coordination subproblem. However, the minimization problem for $\mathbf{U}_2$ would be insoluble due to the rank deficiency of matrix $\mathbf{K}_2$. Since the final form of the design decomposition method of the present paper will be an EP problem, another argument against the $(\mathbf{U}_1, \mathbf{U}_2)$ decomposition can be made based on the sufficient conditions for the existence of an EP solution (see ref. 4). The existence theorem for an EP solution requires that the solution space for the EP subproblem $\min_{\mathbf{U}_2} \left(1/2\ \mathbf{U}_2^T\mathbf{K}_2\mathbf{U}_2 - \tilde{\mathbf{F}}_2^T\mathbf{U}_2 \right)$, where $\tilde{\mathbf{F}}_2$ here includes interface forces from substructure 1, be bounded. However $\mathbf{U}_2$ is not bounded as seen from the following argument. Because substructure 2 has six rigid body modes, a rigid body matrix $\mathbf{R}_2$ can be formed that consists of the six rigid body modes as column vectors. This rigid body matrix satisfies the condition $\mathbf{K}_2\mathbf{R}_2 = [0]$, thus the vector $\mathbf{R}_2\boldsymbol{\alpha}_2$ added to any solution to this subproblem will not change the potential energy if the vector $\boldsymbol{\alpha}_2$ satisfies the scalar equation $\mathbf{F}_2^T\mathbf{R}_2\boldsymbol{\alpha}_2 = 0$. Since the vector $\boldsymbol{\alpha}_2$ is not otherwise restricted, it (and therefore $\mathbf{U}_2$) is unbounded, thus the conditions for solution existence cannot be satisfied.

From the preceding arguments, any decomposition must explicitly account for the rigid body modes of the substructures. A decomposition that does this follows. Let $\mathbf{U}_2 = \mathbf{u}_2 + \mathbf{R}_2\boldsymbol{\alpha}_2$ with the supplementary condition $\mathbf{R}_2^T\mathbf{u}_2 = \mathbf{0}$. The minimization problem given

by statement (3) then becomes

$$\min_{(\mathbf{U}_1,\mathbf{u}_2,\alpha_2)} \left(\frac{1}{2}\mathbf{U}_1^T\mathbf{K}_1\mathbf{U}_1 + \frac{1}{2}\mathbf{u}_2^T\mathbf{K}_2\mathbf{u}_2 - \mathbf{F}_1^T\mathbf{U}_1 - \mathbf{F}_2^T(\mathbf{u}_2 + \mathbf{R}_2\alpha_2)\right) \quad (4)$$

$$\mathbf{B}_1\mathbf{U}_1 + \mathbf{B}_2(\mathbf{u}_2 + \mathbf{R}_2\alpha_2) = \mathbf{0}$$

$$\mathbf{R}_2^T\mathbf{u}_2 = \mathbf{0}$$

where the condition $\mathbf{K}_2\mathbf{R}_2 = [0]$ has been utilized, and the supplementary condition has been added to the problem given by statement (3). The necessary conditions for the structural-response problem given by statement (4) are

$$\mathbf{K}_1\mathbf{U}_1 - \mathbf{F}_1 + \mathbf{B}_1^T\lambda = \mathbf{0}$$

$$\tilde{\mathbf{K}}_2 \begin{bmatrix} \mathbf{u}_2 \\ - \\ \mu \end{bmatrix} - \begin{bmatrix} \mathbf{F}_2 - \mathbf{B}_2^T\lambda \\ \hline \mathbf{0} \end{bmatrix} = \mathbf{0} \quad (5)$$

$$\mathbf{R}_2^T(\mathbf{F}_2 - \mathbf{B}_2^T\lambda) = \mathbf{0}$$

$$\mathbf{B}_1\mathbf{U}_1 + \mathbf{B}_2(\mathbf{u}_2 + \mathbf{R}_2\alpha_2) = \mathbf{0}$$

where λ are the Lagrange multipliers for the first constraint in statement (4), μ are the Lagrange multipliers for the second constraint in statement (4), and the matrix $\tilde{\mathbf{K}}_2$ is the augmented stiffness matrix given by

$$\tilde{\mathbf{K}}_2 = \left[\begin{array}{c|c} \mathbf{K}_2 & \mathbf{R}_2 \\ \hline \mathbf{R}_2^T & [0] \end{array}\right] \quad (6)$$

Because the matrices $\mathbf{B}_i$ in necessary conditions (5) are Boolean, the Lagrange multipliers λ are simply the interface forces between the substructures. Using the second equation in necessary conditions (5), the condition $\mathbf{R}_2^T\mathbf{K}_2 = [0]$, and the fact that the columns of $\mathbf{R}_2$ are linearly independent, the third equation in necessary conditions (5) implies that the Lagrange multipliers μ are equal to zero.

Two structural-response EP subproblems that are implied by necessary conditions (5) are those with necessary conditions

$$\mathbf{K}_1\mathbf{U}_1 = \mathbf{F}_1 - \mathbf{B}_1^T\lambda \quad (7)$$

and

$$\tilde{\mathbf{K}}_2 \begin{bmatrix} \mathbf{u}_2 \\ - \\ \mu \end{bmatrix} = \begin{bmatrix} \mathbf{F}_2 - \mathbf{B}_2^T\lambda \\ \hline \mathbf{0} \end{bmatrix} \quad (8)$$

which are solved for $\mathbf{U}_1$ and $(\mathbf{u}_2, \mu)$, respectfully. The structural-response coordination EP subproblem that determines λ and α_2 is obtained by substituting the solutions of equations (7) and (8) into the last two equations in necessary conditions (5)

$$\mathbf{M}\begin{bmatrix} \lambda \\ - \\ \alpha_2 \end{bmatrix} = \left[\begin{array}{c} \mathbf{B}_1\mathbf{K}_1^{-1}\mathbf{F}_1 + \\ \left[\mathbf{B}_2 \,|\, [0]\right]\tilde{\mathbf{K}}_2^{-1}\left[\mathbf{F}_2^T \,|\, \mathbf{0}^T\right]^T \\ \hline -\mathbf{R}_2^T\mathbf{F}_2 \end{array}\right] \quad (9)$$

where the matrix $\mathbf{M}$ is given by

$$\mathbf{M} = \left[\begin{array}{c|c} \mathbf{B}_1\mathbf{K}_1^{-1}\mathbf{B}_1^T + \left[\mathbf{B}_2 \,|\, [0]\right]\tilde{\mathbf{K}}_2^{-1}\left[\mathbf{B}_2 \,|\, [0]\right]^T & -\mathbf{B}_2\mathbf{R}_2 \\ \hline -(\mathbf{B}_2\mathbf{R}_2)^T & [0] \end{array}\right] \quad (10)$$

The EP subproblem with necessary conditions given by equation (8) includes the constraint that $\mathbf{u}_2$ has no rigid body modes. This constraint essentially bounds the solution space, and thus satisfies the requirement for existence of a solution. The existence of a unique solution to equation (8) is guaranteed from the linear independence of the columns of matrix $\tilde{\mathbf{K}}_2$ which results from augmenting the stiffness matrix $\mathbf{K}_2$ with the rigid body modes $\mathbf{R}_2$ that are in its null space. Thus, the structural response (i.e., nodal displacements) can be solved using the following steps: 1) factor the matrices $\mathbf{K}_1$ and $\tilde{\mathbf{K}}_2$ that are used in equations (7) and (8); 2) use these factored matrices to formulate the matrix $\mathbf{M}$ and the right hand side of equation (9); 3) solve equation (9) for λ and α_2; and 4) solve equations (7) and (8) for $\mathbf{U}_1$ and $\mathbf{u}_2$, respectively.

Structural Optimization with Constraints Local to the Substructures

In this section, the structural optimization problem is decomposed into a set of EP subproblems that are used to perform the optimization, and the related structural analysis, of each substructure. Only structural-sizing design variables, herein termed sizing variables, such as plate thickness or beam section properties, are considered in the present derivation. Also, the present derivation only considers constraints local to the substructures, that is, a constraint relation must explicitly depend on the sizing variables and structural response of only one substructure. The two-substructure wing example from the previous section will be used to demonstrate the present method of decomposition; however, this method is extended to multiple substructures in the appendix. The decomposition is derived from the necessary conditions of a simultaneous analysis and design formulation (ref. 5). In the present

simultaneous analysis and design formulation, minimum weight is the design goal, both the structural displacements and the sizing variables are utilized as design variables, and the optimization constraints are the equations governing structural response (treated as equality constraints) as well as the usual inequality constraints that ensure that the design meets the strength, buckling, and other design requirements. The present method has the following features: 1) the optimization of each substructure is independent and can be done in parallel (although the overall optimization procedure is still iterative); 2) the resulting design is optimal; 3) the objective function of each substructure optimization is the weight of the substructure plus a penalty term derived from an structural-sizing coordination subproblem; 4) the structural-sizing coordination subproblem is a matrix equation that uses the same matrix $\mathbf{M}$ as in the structural-response coordination subproblem (equation (10)); and 5) each substructure optimization depends directly on only the sizing variables and displacements of the substructure being optimized.

The local constraint function vectors for substructures 1 and 2 will be denoted as $\mathbf{g}_1(\mathbf{v}_1, \mathbf{U}_1)$ and $\mathbf{g}_2(\mathbf{v}_2, \mathbf{U}_2)$, respectively. The vectors $\mathbf{v}_1$ and $\mathbf{v}_2$ are vectors of sizing variables for the two substructures. In general, the constraint function vector for the second substructure is expressed by the relation $\mathbf{g}_2(\mathbf{v}_2, \mathbf{U}_2) = \mathbf{g}_2(\mathbf{v}_2, \mathbf{u}_2 + \mathbf{R}_2\boldsymbol{\alpha}_2)$, but, because stress is invariant with respect to rigid body motions, it simplifies to $\mathbf{g}_2(\mathbf{v}_2, \mathbf{u}_2)$ for local strength and buckling constraints. The approach to forming the decomposed optimization problem is as follows: 1) express the optimal design problem as a simultaneous analysis and design problem using necessary conditions (5) for the previously derived structural-response method as additional constraints; 2) determine the necessary condition equations for this simultaneous analysis and design problem; 3) reduce the necessary condition equations for the sizing variables of each substructure to a form which has a contribution from the local substructure and a term representing coupling to other substructures; and 4) treat these reduced necessary condition equations as if they are from an EP problem, and transform the reduced necessary condition equations to a set of EP subproblems and a structural-sizing coordination subproblem.

Simultaneous Analysis and Design Formulation. The optimal design problem is posed using the simultaneous analysis and design approach where necessary conditions (5) that describe the structural response are formulated as constraints. Thus, the problem to be solved is given by

$$
\begin{aligned}
\min_{(\mathbf{v}_1,\mathbf{v}_2,\mathbf{U}_1,\mathbf{u}_2,\boldsymbol{\alpha}_2,\boldsymbol{\lambda},\boldsymbol{\mu})} \quad & W_1(\mathbf{v}_1)+W_2(\mathbf{v}_2) \\
& \mathbf{g}_1(\mathbf{v}_1, \mathbf{U}_1) \le \mathbf{0} \\
& \mathbf{g}_2(\mathbf{v}_2, \mathbf{u}_2 + \mathbf{R}_2\boldsymbol{\alpha}_2) \le \mathbf{0} \\
& \mathbf{K}_1(\mathbf{v}_1)\mathbf{U}_1 - \mathbf{F}_1 + \mathbf{B}_1^T\boldsymbol{\lambda} = \mathbf{0} \\
& \tilde{\mathbf{K}}_2(\mathbf{v}_2) \begin{bmatrix} \mathbf{u}_2 \\ - \\ \boldsymbol{\mu} \end{bmatrix} - \begin{bmatrix} \mathbf{F}_2 - \mathbf{B}_2^T\boldsymbol{\lambda} \\ \text{------} \\ \mathbf{0} \end{bmatrix} = \mathbf{0} \\
& \mathbf{B}_1\mathbf{U}_1 + \mathbf{B}_2(\mathbf{u}_2 + \mathbf{R}_2\boldsymbol{\alpha}_2) = \mathbf{0} \\
& \boldsymbol{\mu} = \mathbf{0}
\end{aligned}
\tag{11}
$$

where the weights W_1 and W_2, and the stiffness matrices of the two substructures are explicit functions of the sizing variables as shown, and the third equation in necessary conditions (5) is replaced with the equivalent condition $\boldsymbol{\mu} = \mathbf{0}$.

Necessary Conditions. The Lagrangian function for this optimization problem is

$$
\begin{aligned}
L =& W_1(\mathbf{v}_1) + W_2(\mathbf{v}_2) + \boldsymbol{\gamma}_1^T\mathbf{g}_1(\mathbf{v}_1, \mathbf{U}_1) \\
& + \boldsymbol{\gamma}_2^T\mathbf{g}_2(\mathbf{v}_2, \mathbf{u}_2 + \mathbf{R}_2\boldsymbol{\alpha}_2) \\
& + \boldsymbol{\nu}_1^T\left(\mathbf{K}_1(\mathbf{v}_1)\mathbf{U}_1 - \mathbf{F}_1 + \mathbf{B}_1^T\boldsymbol{\lambda}\right) \\
& + \boldsymbol{\nu}_2^T\left(\tilde{\mathbf{K}}_2(\mathbf{v}_2) \begin{bmatrix} \mathbf{u}_2 \\ - \\ \boldsymbol{\mu} \end{bmatrix} - \begin{bmatrix} \mathbf{F}_2 - \mathbf{B}_2^T\boldsymbol{\lambda} \\ \text{------} \\ \mathbf{0} \end{bmatrix}\right) \\
& + \boldsymbol{\delta}^T\left(\mathbf{B}_1\mathbf{U}_1 + \mathbf{B}_2(\mathbf{u}_2 + \mathbf{R}_2\boldsymbol{\alpha}_2)\right) + \boldsymbol{\eta}_2^T\boldsymbol{\mu}
\end{aligned}
\tag{12}
$$

In this definition, the quantities $\boldsymbol{\gamma}_i$, $\boldsymbol{\nu}_i$, $\boldsymbol{\delta}$, and $\boldsymbol{\eta}$ are Lagrange multipliers for the constraints in statement (11). Taking the derivatives of the Lagrangian function defined in equation (12) with respect to the design variables of the optimization problem in statement (11) gives the following equations which are part of the set

of necessary conditions

$$\begin{aligned}
\frac{\partial W_1}{\partial \mathbf{v}_1} + \boldsymbol{\gamma}_1^T \frac{\partial \mathbf{g}_1}{\partial \mathbf{v}_1} + \boldsymbol{\nu}_1{}^T \frac{\partial \mathbf{K}_1 \mathbf{U}_1}{\partial \mathbf{v}_1} &= \mathbf{0}^T \\
\frac{\partial W_2}{\partial \mathbf{v}_2} + \boldsymbol{\gamma}_2^T \frac{\partial \mathbf{g}_2}{\partial \mathbf{v}_2} + \boldsymbol{\nu}_2^T \frac{\partial \tilde{\mathbf{K}}_2 \left[\mathbf{u}_2^T \mid \mathbf{0}^T \right]^T}{\partial \mathbf{v}_2} &= \mathbf{0}^T \\
\boldsymbol{\gamma}_1^T \frac{\partial \mathbf{g}_1}{\partial \mathbf{U}_1} + \boldsymbol{\nu}_1^T \mathbf{K}_1 + \boldsymbol{\delta}^T \mathbf{B}_1 &= \mathbf{0}^T \\
\boldsymbol{\gamma}_2^T \frac{\partial \mathbf{g}_2}{\partial \mathbf{u}_2} + \boldsymbol{\nu}_2^T \tilde{\mathbf{K}}_2 \left[\begin{array}{c} I_{p \times p} \\ \hline [0] \end{array} \right] + \boldsymbol{\delta}^T \mathbf{B}_2 &= \mathbf{0}^T \\
\boldsymbol{\gamma}_2^T \frac{\partial \mathbf{g}_2}{\partial \mathbf{u}_2} \mathbf{R}_2 + \boldsymbol{\delta}^T \mathbf{B}_2 \mathbf{R}_2 &= \mathbf{0}^T \\
\boldsymbol{\nu}_1^T \mathbf{B}_1^T + \boldsymbol{\nu}_2^T \left[\begin{array}{c} \mathbf{B}_2^T \\ \hline [0] \end{array} \right] &= \mathbf{0}^T \\
\boldsymbol{\nu}_2^T \tilde{\mathbf{K}}_2 \left[\begin{array}{c} [0] \\ \hline I_{q \times q} \end{array} \right] + \boldsymbol{\eta}_2^T &= \mathbf{0}^T
\end{aligned} \tag{13}$$

where $I_{r \times r}$ is the identity matrix of dimension r, p is the number of degrees-of-freedom for the structural response of substructure 2, q is the number of rigid body modes for substructure 2, and the relation $\boldsymbol{\mu} = \mathbf{0}$ has been utilized.

The sensitivity relations for equations (7) and (8) with respect to the sizing variables will be necessary for continuing the derivation. These relations are expressed by

$$\begin{aligned}
\frac{\partial \mathbf{K}_1 \mathbf{U}_1}{\partial \mathbf{v}_1} + \mathbf{K}_1 \frac{d\mathbf{U}_1}{d\mathbf{v}_1} + \mathbf{B}_1^T \frac{d\boldsymbol{\lambda}}{d\mathbf{v}_1} &= [0] \\
\frac{\partial \tilde{\mathbf{K}}_2 \left[\mathbf{u}_2^T \mid \mathbf{0}^T \right]^T}{\partial \mathbf{v}_2} + \tilde{\mathbf{K}}_2 \left[\begin{array}{c} \frac{d\mathbf{u}_2}{d\mathbf{v}_2} \\ \hline [0] \end{array} \right] + \left[\begin{array}{c} \mathbf{B}_2^T \frac{d\boldsymbol{\lambda}}{d\mathbf{v}_2} \\ \hline [0] \end{array} \right] &= [0]
\end{aligned} \tag{14}$$

Using equations (14), the sensitivity derivatives of the structural response holding the interactions between the substructures fixed (i.e., fixed $\boldsymbol{\lambda}$) are

$$\begin{aligned}
\left. \frac{d\mathbf{U}_1}{d\mathbf{v}_1} \right|_\lambda &= -\mathbf{K}_1^{-1} \frac{\partial \mathbf{K}_1 \mathbf{U}_1}{\partial \mathbf{v}_1} \\
\left[\begin{array}{c} \left. \frac{d\mathbf{u}_2}{d\mathbf{v}_2} \right|_\lambda \\ \hline \left. \frac{d\boldsymbol{\mu}}{d\mathbf{v}_2} \right|_\lambda \end{array} \right] &= -\tilde{\mathbf{K}}_2^{-1} \frac{\partial \tilde{\mathbf{K}}_2 \left[\mathbf{u}_2^T \mid \mathbf{0}^T \right]^T}{\partial \mathbf{v}_2}
\end{aligned} \tag{15}$$

Although the total derivative $d\boldsymbol{\mu}/d\mathbf{v}_2$ is identically equal to zero as indicated in equations (14), the restricted derivative $d\boldsymbol{\mu}/d\mathbf{v}_2|_\lambda$ in definitions (15) is not.

Reduction of Necessary Conditions. Proceeding with the reduction of the necessary conditions, the Lagrange multipliers $\boldsymbol{\nu}_1$ are obtained from the third equation in necessary conditions (13)

$$\boldsymbol{\nu}_1^T = -\left(\boldsymbol{\gamma}_1^T \frac{\partial \mathbf{g}_1}{\partial \mathbf{U}_1} + \boldsymbol{\delta}^T \mathbf{B}_1 \right) \mathbf{K}_1^{-1} \tag{16}$$

and the Lagrange multipliers $\boldsymbol{\nu}_2$ are obtained by combining the fourth and last equations in necessary conditions (13)

$$\boldsymbol{\nu}_2^T = -\left[\boldsymbol{\gamma}_2^T \frac{\partial \mathbf{g}_2}{\partial \mathbf{u}_2} + \boldsymbol{\delta}^T \mathbf{B}_2 \;\mid\; \boldsymbol{\eta}_2^T \right] \tilde{\mathbf{K}}_2^{-1} \tag{17}$$

Substituting equations (16) and (17) into the first and second equations of necessary conditions (13), respectively, and utilizing definitions (15), gives two of the reduced necessary conditions

$$\begin{aligned}
\frac{\partial W_1}{\partial \mathbf{v}_1} + \boldsymbol{\gamma}_1^T \left(\frac{\partial \mathbf{g}_1}{\partial \mathbf{v}_1} + \frac{\partial \mathbf{g}_1}{\partial \mathbf{U}_1} \left. \frac{d\mathbf{U}_1}{d\mathbf{v}_1} \right|_\lambda \right) \\
+ \boldsymbol{\delta}^T \mathbf{B}_1 \left. \frac{d\mathbf{U}_1}{d\mathbf{v}_1} \right|_\lambda &= \mathbf{0}^T \\
\frac{\partial W_2}{\partial \mathbf{v}_2} + \boldsymbol{\gamma}_2^T \left(\frac{\partial \mathbf{g}_2}{\partial \mathbf{v}_2} + \frac{\partial \mathbf{g}_2}{\partial \mathbf{u}_2} \left. \frac{d\mathbf{u}_2}{d\mathbf{v}_2} \right|_\lambda \right) \\
+ \boldsymbol{\delta}^T \mathbf{B}_2 \left. \frac{d\mathbf{u}_2}{d\mathbf{v}_2} \right|_\lambda + \boldsymbol{\eta}_2^T \left. \frac{d\boldsymbol{\mu}}{d\mathbf{v}_2} \right|_\lambda &= \mathbf{0}^T
\end{aligned} \tag{18}$$

The final step in reducing the necessary condition equations is to find expressions for $\boldsymbol{\delta}$ and $\boldsymbol{\eta}_2$. Substituting equations (16) and (17) into the sixth equation in necessary conditions (13), and defining the quantity $\tilde{\boldsymbol{\eta}}_2 = -\left[\mathbf{R}_2^T \mathbf{R}_2 \right]^{-1} \boldsymbol{\eta}_2$ which implies that $-\tilde{\boldsymbol{\eta}}_2^T \left[\mathbf{R}_2^T \mid [0] \right] = \boldsymbol{\eta}_2^T \left[[0] \mid I_{q \times q} \right] \tilde{\mathbf{K}}_2^{-1}$, the following expression is obtained

$$\begin{aligned}
\left[\begin{array}{c} \boldsymbol{\delta} \\ \hline \tilde{\boldsymbol{\eta}}_2 \end{array} \right]^T \left[\begin{array}{c} \mathbf{B}_1 \mathbf{K}_1^{-1} \mathbf{B}_1^T + \left[\mathbf{B}_2 \mid [0] \right] \tilde{\mathbf{K}}_2^{-1} \left[\mathbf{B}_2 \mid [0] \right]^T \\ \hline -(\mathbf{B}_2 \mathbf{R}_2)^T \end{array} \right] \\
= -\left[\boldsymbol{\gamma}_2^T \frac{\partial \mathbf{g}_2}{\partial \mathbf{u}_2} \mid \mathbf{0}^T \right] \tilde{\mathbf{K}}_2^{-1} \left[\mathbf{B}_2 \mid [0] \right]^T \\
- \boldsymbol{\gamma}_1^T \frac{\partial \mathbf{g}_1}{\partial \mathbf{U}_1} \mathbf{K}_1^{-1} \mathbf{B}_1^T
\end{aligned} \tag{19}$$

Combining this equation with the fifth equation in necessary conditions (13) gives the following equation

for $\boldsymbol{\delta}$ and $\tilde{\boldsymbol{\eta}}_2$

$$\mathbf{M}\begin{bmatrix}\boldsymbol{\delta}\\ -\\ \tilde{\boldsymbol{\eta}}_2\end{bmatrix} = \begin{bmatrix} -\left[\mathbf{B}_2 \mid [0]\right]\tilde{\mathbf{K}}_2^{-1}\left[\boldsymbol{\gamma}_2^T\dfrac{\partial \mathbf{g}_2}{\partial \mathbf{u}_2} \mid \mathbf{0}^T\right]^T \\ -\mathbf{B}_1\mathbf{K}_1^{-1}\left(\boldsymbol{\gamma}_1^T\dfrac{\partial \mathbf{g}_1}{\partial \mathbf{U}_1}\right)^T \\ \hline \left(\boldsymbol{\gamma}_2^T\dfrac{\partial \mathbf{g}_2}{\partial \mathbf{u}_2}\mathbf{R}_2\right)^T \end{bmatrix} \tag{20}$$

The matrix $\mathbf{M}$ in equation (20) is the same matrix defined in equation (10).

Transformation to EP Subproblems. The reduced necessary condition equations (18) can be transformed into EP subproblems having these equations as their necessary conditions. Four types of subproblems result: structural-response subproblems, structural-sizing subproblems, a structural-response coordination subproblem, and a structural-sizing coordination subproblem. Only the structural-sizing subproblems are actually transformed into constrained-minimization problems. The first step in these transformations is to define approximate models for $\mathbf{U}_1$ and $\mathbf{u}_2$ that do not consider coupling of the substructures. To fulfill the EP necessary conditions, the approximate models for $\mathbf{U}_1$ and $\mathbf{u}_2$ must have the same values and the same sensitivity derivatives as the exact responses for the optimal values of the sizing variables. To solve the individual subproblems efficiently, only simple models that are explicit functions of the subproblem sizing variables are considered. Although many approximate models are possible (see ref. 6), a simple first-order Taylor series is used in the present derivation. The approximate models are defined by

$$\begin{aligned}\mathbf{U}_1^A(\mathbf{v}_1) &= \left.\frac{d\mathbf{U}_1}{d\mathbf{v}_1}\right|_\lambda (\mathbf{v}_1 - \hat{\mathbf{v}}_1) + \hat{\mathbf{U}}_1 \\ \mathbf{u}_2^A(\mathbf{v}_2) &= \left.\frac{d\mathbf{u}_2}{d\mathbf{v}_2}\right|_\lambda (\mathbf{v}_2 - \hat{\mathbf{v}}_2) + \hat{\mathbf{u}}_2\end{aligned} \tag{21}$$

where the displacements with the caret accents and the restricted derivatives in equations (21) are calculated at specific values of the sizing variables denoted by $\hat{\mathbf{v}}_i$. Also for compactness, the dependence on these previously calculated values are not explicitly given in the function arguments. With these definitions, two EP structural-sizing subproblems can be formed that have reduced necessary condition equations (18) as their necessary conditions. The EP subproblem for the first substructure is developed from the first equation in equations (18), and is given by the statement

$$\begin{aligned}&\min_{\mathbf{v}_1} W_1(\mathbf{v}_1) + \boldsymbol{\delta}^T\mathbf{B}_1\mathbf{U}_1^A(\mathbf{v}_1) \\ &\mathbf{g}_1(\mathbf{v}_1, \mathbf{U}_1^A(\mathbf{v}_1)) \le \mathbf{0}\end{aligned} \tag{22}$$

where the Lagrange multipliers for $\mathbf{g}_1$ are $\boldsymbol{\gamma}_1$. Similarly, the structural-sizing subproblem for the second substructure is developed from the second equation in reduced necessary conditions (18), and is given by the statement

$$\begin{aligned}&\min_{\mathbf{v}_2} W_2(\mathbf{v}_2) + \boldsymbol{\delta}^T\mathbf{B}_2\mathbf{u}_2^A(\mathbf{v}_2) + \boldsymbol{\eta}_2^T\left.\frac{d\boldsymbol{\mu}}{d\mathbf{v}_2}\right|_\lambda \mathbf{v}_2 \\ &\mathbf{g}_2(\mathbf{v}_2, \mathbf{u}_2^A(\mathbf{v}_2) + \mathbf{R}_2\boldsymbol{\alpha}_2) \le \mathbf{0}\end{aligned} \tag{23}$$

where the Lagrange multipliers for $\mathbf{g}_2$ are $\boldsymbol{\gamma}_2$. Equation (20) is the coordination subproblem that determines the penalty coefficients $\boldsymbol{\delta}$ and $\boldsymbol{\eta}_2 = -\mathbf{R}_2^T\mathbf{R}_2\,\tilde{\boldsymbol{\eta}}_2$ by utilizing the Lagrange multipliers determined from solving the subproblems given by statements (22) and (23). The structural response is given by solving equations (7), (8), and (9), and the restricted derivatives are given by definitions (15).

Discussion

Summarizing the salient features of the present method, a set of interacting EP subproblems, each associated with a particular substructure except for two coordination subproblems, is iteratively solved until the equilibrium solution is achieved. The structural-response subproblem for each substructure is independent of the structural response of the rest of the structure because the coupling of the structural-response subproblems is achieved using a set of Lagrange multipliers which represent forces between the substructures. A computational advantage is obtained because the expensive factorization of matrices can be done in parallel for each substructure. The Lagrange multipliers representing the forces between substructures, and the substructure rigid body modes are determined within a structural-response coordination subproblem. The optimization of substructures that have constraints that are local to a substructure is accomplished in structural-sizing subproblems in a manner so that the individual substructure optimizations are independent of each other, and can be accomplished in parallel. The computational efficiency is enhanced because the only structural-response sensitivity derivative information required is local to the substructure being optimized. The penalty terms in each structural-sizing subproblem that represent the coupling of the substructure optimizations ensure that the overall design is optimal. Additional computational advantages may be

accrued because the calculation of the coefficients for these penalty terms is done in a structural-sizing coordination subproblem that utilizes the same matrix utilized in the structural-response coordination subproblem. The approximate updated sensitivity derivative method reported in reference 7 may prove to enhance further the computational efficiency of the method.

Several aspects of the decomposition method require further research. One aspect that needs attention is the translation of the theory derived in the present report into a viable numerical algorithm. This translation implies the need for methods to form and factor the augmented stiffness matrices of the substructures, and to form and factor the coupling matrix $\mathbf{M}$ that is necessary for calculating the substructure interface forces and rigid body modes, and the penalty terms of the structural-sizing subproblems. In addition, although several EP theorems may prove existence of a solution, in practice the substructural optimizations will require rational selections of move limits on the sizing variables, and a strategy for dealing with subproblems having no feasible solution (a modification of the method described in reference 6 that includes a constraint violation penalty for each structural-sizing subproblem is presently envisioned). Also, the stability of the solution process, and the convergence to the equilibrium solution needs to be studied. Another area of interest is the extension of the method to constraints that are more general than constraints which are local to a substructure. The utilization of parallel computers to implement the method also requires investigation.

Conclusions

A new method for structural analysis and structural optimization utilizing a substructure-based decomposition has been derived in detail for two substructures and extended for multiple substructures. Because the starting point for the decomposition is a simultaneous design and analysis formulation of the design problem, the solution to the resulting decomposed system of subproblems is optimal. The final form of the design decomposition is a set of loosely coupled subproblems that define an Equilibrium Programming (EP) problem. Thus, existence of a solution to the decomposed system can be studied utilizing EP existence theorems. All of the structural-response subproblems for the substructures can be solved independently of each other, as can all of the structural-sizing subproblems. Thus, significant potential exists for the development of a parallel solution method that utilizes this decomposition of the optimal design problem to reduce the solution time for large problems.

Appendix

Extension of Method to Multiple Substructures

Assume that there are n substructures, and that m substructures ($0 \leq m \leq n$) have rigid body modes when separated from the rest of the structure. The n_i displacement degrees-of-freedom of substructure i are denoted by $\mathbf{U}_i = (U_{i1}, \ldots, U_{in_i})^T$. The substructures having rigid body modes are ordered to be the last m substructures. These substructures have displacements denoted by $\mathbf{U}_i = \mathbf{u}_i + \mathbf{R}_i\boldsymbol{\alpha}_i$ where $\mathbf{R}_i$ is the matrix containing the rigid body modes of substructure i, and $\mathbf{R}_i^T\mathbf{u}_i = \mathbf{0}$. The equivalencing of degrees-of-freedom at common interface nodes in the different substructures is represented by the set A of n^I 4-tuples defined by $A = \{\,(j,k,p,q) \mid j < k \text{ and } U_{jp} \equiv U_{kq}\,\}$. In the definition of set A, redundancies in the equivalencing of degrees-of-freedom are omitted. For example, a degree-of-freedom shared by three substructures need only be equivalenced between two pairs of substructures, not all three pair-wise combinations. The compatibility constraint equations (i.e., the equations that enforce compatibility between the substructures) are defined by assigning an order to the elements of set A that corresponds to the order of the compatibility constraint equations. Thus, the r^{th} compatibility constraint equation will depend on degrees-of-freedom in substructure j if either the first or second element of the r^{th} 4-tuple in A is j. These compatibility constraint equations are expressed explicitly by defining the signed Boolean matrices $\mathbf{B}_j$ for $j = 1, \ldots, n$ which have dimensions $n^I \times n_j$. Matrix $\mathbf{B}_j$ has a 1 at location rp if the r^{th} 4-tuple in A has the components $(j, \cdot, p, \cdot)$, and it has a -1 at location rq if the r^{th} 4-tuple in A has the components $(\cdot, j, \cdot, q)$. Otherwise, the entries in matrix $\mathbf{B}_j$ are zero. Thus, the compatibility constraint equations for all the substructures are symbolically represented by the system of n^I equations:

$$\sum_{i=1}^{n} \mathbf{B}_i\mathbf{U}_i = \mathbf{0} \tag{A1}$$

The definition of the Boolean matrix $\mathbf{B}_j$ in the present section reduces to the previous definition of the Boolean matrix for the case of only two substructures.

Decomposition of the Structural Response

Utilizing the previously described definitions, the minimization problem for the structural response given by statement (4) generalizes to:

$$\min_{\substack{(\mathbf{U}_1,\ldots,\mathbf{U}_{n-m},\\ \mathbf{u}_{n-m+1},\ldots,\mathbf{u}_n,\\ \boldsymbol{\alpha}_{n-m+1},\ldots,\boldsymbol{\alpha}_n)}} \sum_{i=1}^{n-m}\left(\frac{1}{2}\mathbf{U}_i^T\mathbf{K}_i\mathbf{U}_i - \mathbf{F}_i^T\mathbf{U}_i\right) + \sum_{i=n-m+1}^{n}\left(\frac{1}{2}\mathbf{u}_i^T\mathbf{K}_i\mathbf{u}_i - \mathbf{F}_i^T(\mathbf{u}_i + \mathbf{R}_i\boldsymbol{\alpha}_i)\right)$$

$$\sum_{i=1}^{n-m}\mathbf{B}_i\mathbf{U}_i + \sum_{j=n-m+1}^{n}\mathbf{B}_j(\mathbf{u}_j + \mathbf{R}_j\boldsymbol{\alpha}_j) = \mathbf{0} \tag{A2}$$

$$\mathbf{R}_i\mathbf{u}_i = \mathbf{0} \qquad \text{for} \quad i = n-m+1, \ldots, n$$

The necessary conditions for the minimization problem given by statement ($A2$) are

$$\mathbf{K}_i\mathbf{U}_i - \mathbf{F}_i + \mathbf{B}_i^T\boldsymbol{\lambda} = \mathbf{0} \qquad \text{for} \quad i = 1, \ldots, m-n$$

$$\tilde{\mathbf{K}}_i \begin{bmatrix} \mathbf{u}_i \\ - \\ \boldsymbol{\mu}_i \end{bmatrix} - \begin{bmatrix} \mathbf{F}_i - \mathbf{B}_i^T\boldsymbol{\lambda} \\ ----- \\ \mathbf{0} \end{bmatrix} = \mathbf{0} \qquad \text{for} \quad i = n-m+1, \ldots, n \tag{A3}$$

$$\mathbf{R}_i^T(\mathbf{F}_i - \mathbf{B}_i^T\boldsymbol{\lambda}) = \mathbf{0} \qquad \text{for} \quad i = n-m+1, \ldots, n$$

along with the first constraint equation given in statement ($A2$). Here $\boldsymbol{\lambda}$ are the Lagrange multipliers corresponding to the first constraint equation in statement ($A2$), $\boldsymbol{\mu}_i$ are the Lagrange multipliers for the last constraint equation

in statement $(A2)$, and the matrix $\tilde{\mathbf{K}}_i$ for $i = n-m+1,\ldots,n$ is the augmented stiffness matrix given by

$$\tilde{\mathbf{K}}_i = \left[\begin{array}{c|c} \mathbf{K}_i & \mathbf{R}_i \\ \hline \mathbf{R}_i^T & [0] \end{array}\right] \tag{A4}$$

Using the second equation in necessary conditions $(A3)$, the condition $\mathbf{R}_i^T\mathbf{K}_i = [0]$ for $i = n-m+1,\ldots,n$, and the fact that the columns of $\mathbf{R}_i$ are linearly independent, the last equation in necessary conditions $(A3)$ implies that the Lagrange multipliers $\boldsymbol{\mu}_i$ are equal to zero. The structural responses $\mathbf{U}_i$ for $i = 1,\ldots,n-m$, and $(\mathbf{u}_i, \boldsymbol{\mu}_i)$ for $i = n-m+1,\ldots,n$ are found by solving the first and second equations of necessary conditions $(A3)$, respectively, after the vector $\boldsymbol{\lambda}$ is determined.

The vector $\boldsymbol{\lambda}$ must be determined simultaneously with the rigid body displacements $\boldsymbol{\alpha}_i$ for $i = n-m+1,\ldots,n$. This solution is accomplished by substituting the symbolic solutions for $\mathbf{U}_i$ and $\mathbf{u}_i$ into the compatibility constraint equation in statement $(A2)$, and solving this equation simultaneously with the last equation in necessary conditions $(A3)$. The following matrix equation gives the resulting system:

$$\mathbf{M}\begin{bmatrix} \boldsymbol{\lambda} \\ \boldsymbol{\alpha}_{n-m+1} \\ \boldsymbol{\alpha}_{n-m+2} \\ \vdots \\ \boldsymbol{\alpha}_n \end{bmatrix} = \begin{bmatrix} \sum_{i=1}^{n-m}\mathbf{B}_i\mathbf{K}_i^{-1}\mathbf{F}_i + \sum_{i=n-m+1}^{n}\left[\mathbf{B}_i \,|\, [0]\right]\tilde{\mathbf{K}}_i^{-1}\left[\mathbf{F}_i^T \,|\, \mathbf{0}^T\right]^T \\ -\mathbf{R}_{n-m+1}^T\mathbf{F}_{n-m+1} \\ -\mathbf{R}_{n-m+2}^T\mathbf{F}_{n-m+2} \\ \vdots \\ -\mathbf{R}_n^T\mathbf{F}_n \end{bmatrix} \tag{A5}$$

where the matrix $\mathbf{M}$ is given by

$$\left[\begin{array}{c|c|c|c|c} \sum_{i=1}^{n-m}\mathbf{B}_i\mathbf{K}_i^{-1}\mathbf{B}_i^T + \sum_{i=n-m+1}^{n}\left[\mathbf{B}_i \,|\, [0]\right]\tilde{\mathbf{K}}_i^{-1}\left[\mathbf{B}_i \,|\, [0]\right]^T & -\mathbf{B}_{n-m+1}\mathbf{R}_{n-m+1} & -\mathbf{B}_{n-m+2}\mathbf{R}_{n-m+2} & \cdots & -\mathbf{B}_n\mathbf{R}_n \\ \hline -(\mathbf{B}_{n-m+1}\mathbf{R}_{n-m+1})^T & [0] & [0] & \cdots & [0] \\ \hline -(\mathbf{B}_{n-m+2}\mathbf{R}_{n-m+2})^T & [0] & [0] & \cdots & [0] \\ \hline \vdots & \vdots & \vdots & \ddots & \vdots \\ \hline -(\mathbf{B}_n\mathbf{R}_n)^T & [0] & [0] & \cdots & [0] \end{array}\right] \tag{A6}$$

Equations $(A5)$ and $(A6)$ are the generalizations of equations (9) and (10) for multiple substructures.

Structural Optimization with Constraints Local to the Substructures

As in the two-substructure example, only constraints that are local to the substructures (i.e., that can be expressed using constraint functions of the form $\mathbf{g}_i(\mathbf{v}_i, \mathbf{U}_i)$ for $i = 1,\ldots,n$) are considered in the structural optimization process. The steps utilized when there are multiple substructures are nearly identical to those performed for the two-substructure example. The simultaneous analysis and design formulation is a generalization of the problem of

statement (11)

$$
\begin{aligned}
&\min_{\substack{(\mathbf{v}_1,\ldots,\mathbf{v}_n,\\ \mathbf{U}_1,\ldots,\mathbf{U}_{n-m},\\ \mathbf{u}_{n-m+1},\ldots\mathbf{u}_n,\\ \boldsymbol{\alpha}_{n-m+1},\ldots,\boldsymbol{\alpha}_n,\\ \boldsymbol{\lambda},\boldsymbol{\mu}_{n-m+1},\ldots,\boldsymbol{\mu}_n)}} \quad \sum_{i=1}^{n} W_i(\mathbf{v}_i) \\
&\qquad\qquad \mathbf{g}_i(\mathbf{v}_i,\mathbf{U}_i) \le \mathbf{0} \qquad \text{for} \quad i = 1,\ldots,n-m \\
&\qquad\qquad \mathbf{g}_i(\mathbf{v}_i,\mathbf{u}_i+\mathbf{R}_i\boldsymbol{\alpha}_i) \le \mathbf{0} \qquad \text{for} \quad i = n-m+1,\ldots,n \\
&\qquad\qquad \mathbf{K}_i(\mathbf{v}_i)\mathbf{U}_i - \mathbf{F}_i + \mathbf{B}_i^T\boldsymbol{\lambda} = \mathbf{0} \qquad \text{for} \quad i = 1,\ldots,n-m \\
&\tilde{\mathbf{K}}_i(\mathbf{v}_i)\begin{bmatrix}\mathbf{u}_i\\ -\\ \boldsymbol{\mu}_i\end{bmatrix} - \begin{bmatrix}\mathbf{F}_i - \mathbf{B}_i^T\boldsymbol{\lambda}\\ -----\\ \mathbf{0}\end{bmatrix} = \mathbf{0} \qquad \text{for} \quad i = n-m+1,\ldots,n \\
&\sum_{i=1}^{n-m}\mathbf{B}_i\mathbf{U}_i + \sum_{j=n-m+1}^{n}\mathbf{B}_j(\mathbf{u}_j+\mathbf{R}_j\boldsymbol{\alpha}_j) = \mathbf{0} \\
&\qquad\qquad \boldsymbol{\mu}_i = \mathbf{0} \qquad \text{for} \quad i = n-m+1,\ldots,n
\end{aligned}
\tag{A7}
$$

The Lagrangian function for this optimization problem is defined as

$$
\begin{aligned}
L = &\sum_{i=1}^{n} W_i(\mathbf{v}_i) + \sum_{i=1}^{n-m}\boldsymbol{\gamma}_i^T\mathbf{g}_i(\mathbf{v}_i,\mathbf{U}_i) + \sum_{i=n-m+1}^{n}\boldsymbol{\gamma}_i^T\mathbf{g}_i(\mathbf{v}_i,\mathbf{u}_i+\mathbf{R}_i\boldsymbol{\alpha}_i) \\
&+ \sum_{i=1}^{n-m}\boldsymbol{\nu}_i^T\left(\mathbf{K}_i(\mathbf{v}_i)\mathbf{U}_i - \mathbf{F}_i + \mathbf{B}_i^T\boldsymbol{\lambda}\right) + \sum_{i=n-m+1}^{n}\boldsymbol{\nu}_i^T\left(\tilde{\mathbf{K}}_i(\mathbf{v}_i)\begin{bmatrix}\mathbf{u}_i\\ -\\ \boldsymbol{\mu}_i\end{bmatrix} - \begin{bmatrix}\mathbf{F}_i - \mathbf{B}_i^T\boldsymbol{\lambda}\\ -----\\ \mathbf{0}\end{bmatrix}\right) \\
&+ \boldsymbol{\delta}^T\left(\sum_{i=1}^{n-m}\mathbf{B}_i\mathbf{U}_i + \sum_{j=n-m+1}^{n}\mathbf{B}_j(\mathbf{u}_j+\mathbf{R}_j\boldsymbol{\alpha}_j)\right) + \sum_{i=n-m+1}^{n}\boldsymbol{\eta}_i^T\boldsymbol{\mu}_i
\end{aligned}
\tag{A8}
$$

and the following equations result from the optimality necessary conditions:

$$
\begin{aligned}
&\frac{\partial W_i}{\partial \mathbf{v}_i} + \boldsymbol{\gamma}_i^T\frac{\partial \mathbf{g}_i}{\partial \mathbf{v}_i} + \boldsymbol{\nu}_i{}^T\frac{\partial \mathbf{K}_i\mathbf{U}_i}{\partial \mathbf{v}_i} = \mathbf{0}^T \qquad \text{for} \quad i = 1,\ldots,n-m \\
&\frac{\partial W_i}{\partial \mathbf{v}_i} + \boldsymbol{\gamma}_i^T\frac{\partial \mathbf{g}_i}{\partial \mathbf{v}_i} + \boldsymbol{\nu}_i^T\frac{\partial \tilde{\mathbf{K}}_i\left[\,\mathbf{u}_i^T\,\middle|\,\mathbf{0}^T\,\right]^T}{\partial \mathbf{v}_i} = \mathbf{0}^T \qquad \text{for} \quad i = n-m+1,\ldots,n \\
&\boldsymbol{\gamma}_i^T\frac{\partial \mathbf{g}_i}{\partial \mathbf{U}_i} + \boldsymbol{\nu}_i^T\mathbf{K}_i + \boldsymbol{\delta}^T\mathbf{B}_i = \mathbf{0}^T \qquad \text{for} \quad i = 1,\ldots,n-m \\
&\boldsymbol{\gamma}_i^T\frac{\partial \mathbf{g}_i}{\partial \mathbf{u}_i} + \boldsymbol{\nu}_i^T\tilde{\mathbf{K}}_i\begin{bmatrix}I_{p_i\times p_i}\\ ---\\ [0]\end{bmatrix} + \boldsymbol{\delta}^T\mathbf{B}_i = \mathbf{0}^T \qquad \text{for} \quad i = n-m+1,\ldots,n \\
&\boldsymbol{\gamma}_i^T\frac{\partial \mathbf{g}_i}{\partial \mathbf{u}_i}\mathbf{R}_i + \boldsymbol{\delta}^T\mathbf{B}_i\mathbf{R}_i = \mathbf{0}^T \qquad \text{for} \quad i = n-m+1,\ldots,n \\
&\sum_{i=1}^{n-m}\boldsymbol{\nu}_i^T\mathbf{B}_i^T + \sum_{i=n-m+1}^{n}\boldsymbol{\nu}_i^T\begin{bmatrix}\mathbf{B}_i^T\\ -\\ [0]\end{bmatrix} = \mathbf{0}^T \\
&\boldsymbol{\nu}_i^T\tilde{\mathbf{K}}_i\begin{bmatrix}[0]\\ ---\\ I_{q_i\times q_i}\end{bmatrix} + \boldsymbol{\eta}_i^T = \mathbf{0}^T \qquad \text{for} \quad i = n-m+1,\ldots,n
\end{aligned}
\tag{A9}
$$

where p_i is the number of degrees-of-freedom for the structural response of substructure i, and q_i is the number of rigid body modes in substructure i. This system of equations generalizes necessary conditions (13), and the

constraint $\boldsymbol{\mu}_i = \mathbf{0}$ for $i = n-m+1, \ldots, n$ has been applied. The sensitivity derivatives of the structural response holding the interactions between the substructures fixed (i.e., fixed $\boldsymbol{\lambda}$) are defined as in definitons (15)

$$\begin{aligned} \left.\frac{d\mathbf{U}_i}{d\mathbf{v}_i}\right|_{\lambda} &= -\mathbf{K}_i^{-1}\frac{\partial \mathbf{K}_i \mathbf{U}_i}{\partial \mathbf{v}_i} \qquad \text{for} \quad i = 1, \ldots, n-m \\ \left[\begin{array}{c} \left.\frac{d\mathbf{u}_i}{d\mathbf{v}_i}\right|_{\lambda} \\ \hline \left.\frac{d\boldsymbol{\mu}_i}{d\mathbf{v}_i}\right|_{\lambda} \end{array}\right] &= -\tilde{\mathbf{K}}_i^{-1}\frac{\partial \tilde{\mathbf{K}}_i \left[\, \mathbf{u}_i^T \,|\, \mathbf{0}^T \,\right]^T}{\partial \mathbf{v}_i} \qquad \text{for} \quad i = n-m+1, \ldots, n \end{aligned} \tag{A10}$$

The Lagrange multipliers $\boldsymbol{\nu}_i$ are obtained from the equations in necessary conditions (A9)

$$\begin{aligned} \boldsymbol{\nu}_i^T &= -\left(\boldsymbol{\gamma}_i^T \frac{\partial \mathbf{g}_i}{\partial \mathbf{U}_i} + \boldsymbol{\delta}^T \mathbf{B}_i\right)\mathbf{K}_i^{-1} \qquad \text{for} \quad i = 1, \ldots, n-m \\ \boldsymbol{\nu}_i^T &= -\left[\boldsymbol{\gamma}_i^T \frac{\partial \mathbf{g}_i}{\partial \mathbf{u}_i} + \boldsymbol{\delta}^T \mathbf{B}_i \;\Big|\; \boldsymbol{\eta}_i^T\right]\tilde{\mathbf{K}}_i^{-1} \qquad \text{for} \quad i = n-m+1, \ldots, n \end{aligned} \tag{A11}$$

which are utilized with definitions (A10) to simplify the first two equations in necessary conditions (A9)

$$\begin{aligned} &\frac{\partial W_i}{\partial \mathbf{v}_i} + \boldsymbol{\gamma}_i^T\left(\frac{\partial \mathbf{g}_i}{\partial \mathbf{v}_i} + \frac{\partial \mathbf{g}_i}{\partial \mathbf{U}_i}\left.\frac{d\mathbf{U}_i}{d\mathbf{v}_i}\right|_{\lambda}\right) \\ &\qquad + \boldsymbol{\delta}^T \mathbf{B}_i \left.\frac{d\mathbf{U}_i}{d\mathbf{v}_i}\right|_{\lambda} = \mathbf{0}^T \qquad \text{for} \quad i = 1, \ldots, n-m \\ &\frac{\partial W_i}{\partial \mathbf{v}_i} + \boldsymbol{\gamma}_i^T\left(\frac{\partial \mathbf{g}_i}{\partial \mathbf{v}_i} + \frac{\partial \mathbf{g}_i}{\partial \mathbf{u}_i}\left.\frac{d\mathbf{u}_i}{d\mathbf{v}_i}\right|_{\lambda}\right) \\ &\qquad + \boldsymbol{\delta}^T \mathbf{B}_i \left.\frac{d\mathbf{u}_i}{d\mathbf{v}_i}\right|_{\lambda} + \boldsymbol{\eta}_i^T \left.\frac{d\boldsymbol{\mu}_i}{d\mathbf{v}_i}\right|_{\lambda} = \mathbf{0}^T \qquad \text{for} \quad i = n-m+1, \ldots, n \end{aligned} \tag{A12}$$

As in the case of only two substructures, the final step is to determine values for $\boldsymbol{\delta}$ and $\boldsymbol{\eta}_i$ for $i = n-m+1, \ldots, n$. One equation necessary for determining these quantities is found by substituting expressions for $\boldsymbol{\nu}_i$ from equations (A11) into the sixth equation in necessary conditions (A9). The resulting equation becomes

$$\begin{aligned} &\left[\begin{array}{c} \boldsymbol{\delta} \\ \tilde{\boldsymbol{\eta}}_{n-m+1} \\ \vdots \\ \tilde{\boldsymbol{\eta}}_{n-m+1} \end{array}\right]^T \left[\begin{array}{c} \sum_{i=1}^{n-m} \mathbf{B}_i \mathbf{K}_i^{-1} \mathbf{B}_i^T + \sum_{i=n-m+1}^{n} \left[\mathbf{B}_i \,|\, [0]\right]\tilde{\mathbf{K}}_i^{-1}\left[\mathbf{B}_i \,|\, [0]\right]^T \\ -(\mathbf{B}_{n-m+1}\mathbf{R}_{n-m+1})^T \\ \vdots \\ -(\mathbf{B}_n \mathbf{R}_n)^T \end{array}\right] = \\ &\qquad -\sum_{i=1}^{n-m} \boldsymbol{\gamma}_i^T \frac{\partial \mathbf{g}_i}{\partial \mathbf{U}_i}\mathbf{K}_i^{-1}\mathbf{B}_i^T - \sum_{i=n-m+1}^{n}\left[\boldsymbol{\gamma}_i^T \frac{\partial \mathbf{g}_i}{\partial \mathbf{u}_i} \,|\, \mathbf{0}^T\right]\tilde{\mathbf{K}}_i^{-1}\left[\mathbf{B}_i \,|\, [0]\right]^T \end{aligned} \tag{A13}$$

where the quantities $\tilde{\boldsymbol{\eta}}_i$ for $i = n-m+1, \ldots, n$ are defined by $\tilde{\boldsymbol{\eta}}_i = -\left[\mathbf{R}_i^T \mathbf{R}_i\right]^{-1}\boldsymbol{\eta}_i$. Combining equation (A13) with the fifth equation in necessary conditions (A9) yields the following equation that is solved to determine the values for $\boldsymbol{\delta}$ and $\boldsymbol{\eta}_i$ for $i = n-m+1, \ldots, n$

$$\mathbf{M}\left[\begin{array}{c} \boldsymbol{\delta} \\ \tilde{\boldsymbol{\eta}}_{n-m+1} \\ \vdots \\ \tilde{\boldsymbol{\eta}}_n \end{array}\right] = \left[\begin{array}{c} -\sum_{i=1}^{n-m} \mathbf{B}_i \mathbf{K}_i^{-1}\left(\boldsymbol{\gamma}_i^T \frac{\partial \mathbf{g}_i}{\partial \mathbf{U}_i}\right)^T - \sum_{i=n-m+1}^{n}\left[\mathbf{B}_i \,|\, [0]\right]\tilde{\mathbf{K}}_i^{-1}\left[\boldsymbol{\gamma}_i^T \frac{\partial \mathbf{g}_i}{\partial \mathbf{u}_i} \,|\, \mathbf{0}^T\right]^T \\ \left(\boldsymbol{\gamma}_{n-m+1}^T \frac{\partial \mathbf{g}_{n-m+1}}{\partial \mathbf{u}_{n-m+1}}\mathbf{R}_{n-m+1}\right)^T \\ \vdots \\ \left(\boldsymbol{\gamma}_n^T \frac{\partial \mathbf{g}_n}{\partial \mathbf{u}_n}\mathbf{R}_n\right)^T \end{array}\right] \tag{A14}$$

Formulation of Decomposition as an Equilibrium Programming Problem

The EP subproblems for n substructures are formulated by first defining approximate models for the displacements of the substructures that do not consider coupling between substructures. For example, linear approximate models may be used that have the form

$$\begin{aligned} \mathbf{U}_i^A(\mathbf{v}_i) &= \left.\frac{d\mathbf{U}_i}{d\mathbf{v}_i}\right|_\lambda (\mathbf{v}_i - \hat{\mathbf{v}}_i) + \hat{\mathbf{U}}_i \qquad \text{for} \quad i = 1, \ldots, n-m \\ \mathbf{u}_i^A(\mathbf{v}_i) &= \left.\frac{d\mathbf{u}_i}{d\mathbf{v}_i}\right|_\lambda (\mathbf{v}_i - \hat{\mathbf{v}}_i) + \hat{\mathbf{u}}_i \qquad \text{for} \quad i = n-m+1, \ldots, n \end{aligned} \tag{A15}$$

where the variables having caret accents are as defined previously, and the restricted derivatives are given by definitions (A10). These approximate models are utilized in formulating EP structural-sizing subproblems for the n substructures whose necessary conditions are the same as the equations given in reduced necessary conditions (A12). These structural-sizing subproblems are defined for the substructures having no rigid body modes (i.e., for $i = 1, \ldots, n-m$) as

$$\begin{aligned} &\min_{\mathbf{v}_i} W_1(\mathbf{v}_i) + \boldsymbol{\delta}^T \mathbf{B}_i \mathbf{U}_i^A(\mathbf{v}_i) \\ &\mathbf{g}_i(\mathbf{v}_i, \mathbf{U}_i^A(\mathbf{v}_i)) \leq \mathbf{0} \end{aligned} \tag{A16}$$

The structural-sizing subproblems for the substructures that have rigid body modes (i.e., for $i = n-m+1, \ldots, n$) are defined as

$$\begin{aligned} &\min_{\mathbf{v}_i} W_2(\mathbf{v}_i) + \boldsymbol{\delta}^T \mathbf{B}_i \mathbf{u}_i^A(\mathbf{v}_i) + \boldsymbol{\eta}_i^T \left.\frac{d\boldsymbol{\mu}_i}{d\mathbf{v}_i}\right|_\lambda \mathbf{v}_i \\ &\mathbf{g}_i(\mathbf{v}_i, \mathbf{u}_i^A(\mathbf{v}_i) + \mathbf{R}_i \boldsymbol{\alpha}_i) \leq \mathbf{0} \end{aligned} \tag{A17}$$

The Lagrange multipliers for $\mathbf{g}_i$ in both statements (A16) and (A17) are represented by the vectors $\boldsymbol{\gamma}_i$ which are needed to form the right side of equation (A14). The structural-sizing coordination subproblem given by equation (A14) determines the quantities $\boldsymbol{\delta}$ and $\tilde{\boldsymbol{\eta}}_i$ for $i = n-m+1, \ldots, n$. The terms $\boldsymbol{\eta}_i$ are determined from $\boldsymbol{\eta}_i = -\mathbf{R}_i^T \mathbf{R}_i \, \tilde{\boldsymbol{\eta}}_i$. The structural-response subproblems are given by the first two equations in necessary conditions (A3), and the structural-response coordination subproblem is given by equation (A5).

Acknowledgments

I would like to thank Dr. Raphael Haftka for his many helpful discussions and insights. This research constitutes a portion of the work carried out in conjunction with a doctoral dissertation at the George Washington University.

References

1. Schmit, L. A., and Miura, H.: *Approximation Concepts for Efficient Structural Synthesis.* NASA CR-2552, March 1976.
2. Barthelemy, J.-F. M.: Engineering Design Applications of Multilevel Optimization Methods. *Computer Aided Optimum Design of Structures: Applications*, Proceeding of the first International Conference, Southhampton, UK, June 1989, pp. 113-122.
3. Farhat, C., and Roux, F.-X.: A Method of Finite Element Tearing and Interconnecting and Its Parallel Solution Algorithm. *International Journal for Numerical Methods in Engineering*, vol. 32, 1991, pp. 1205-1227.
4. Scotti, S. J.: Structural Design using Equilibrium Programming. *Proceedings of the AIAA/ASME/ASCE/AHS/ASC 33th Structures, Structural Dynamics, and Materials Conference*, AIAA paper 92-2365, April 13 – 15, 1992.
5. Haftka, R. T.: Simultaneous Analysis and Design. *AIAA Journal*, vol. 23, no. 7, July 1985, pp. 1099-1103.
6. Haftka, R. T., and Gurdal, Z.: *Elements of Structural Optimization*, 3rd edition, Kluwer Academic Publishers, Boston, MA., 1992.
7. Scotti, S. J.: Structural Design Utilizing Updated Approximate Sensitivity Derivatives. *Proceedings of the AIAA/ASME/ASCE/AHS/ASC 34th Structures, Structural Dynamics, and Materials Conference*, AIAA Paper No. 93-1531, April 19 – 21, 1993.

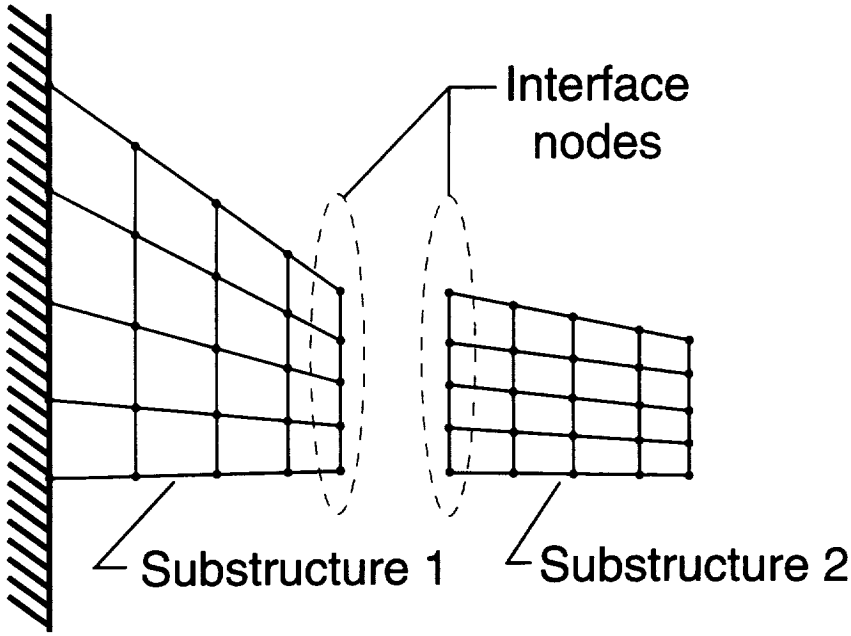

Figure 1. Example wing structural finite element model decomposed into two substructures.

REPORT DOCUMENTATION PAGE

Form Approved
OMB No. 0704-0188

1. AGENCY USE ONLY *(Leave blank)*	2. REPORT DATE	3. REPORT TYPE AND DATES COVERED
	January 1994	Technical Memorandum

4. TITLE AND SUBTITLE
A Structural Design Decomposition Method Utilizing Substructuring

5. FUNDING NUMBERS
WU 505-63-50-08

6. AUTHOR(S)
Stephen J. Scotti

7. PERFORMING ORGANIZATION NAME(S) AND ADDRESS(ES)
NASA Langley Research Center
Hampton, VA 23681-0001

8. PERFORMING ORGANIZATION REPORT NUMBER

9. SPONSORING / MONITORING AGENCY NAME(S) AND ADDRESS(ES)
National Aeronautics and Space Administration
Washington, DC 20546

10. SPONSORING / MONITORING AGENCY REPORT NUMBER
NASA TM-107750

11. SUPPLEMENTARY NOTES

12a. DISTRIBUTION / AVAILABILITY STATEMENT
Unclassified - Unlimited

Subject Category - 39

12b. DISTRIBUTION CODE

13. ABSTRACT *(Maximum 200 words)* The present paper describes a new method of design decomposition for structural analysis and optimization. For this method, the structure is divided into substructures where each substructure has its structural response described by a structural-response subproblem, and its structural sizing determined from a structural-sizing subproblem. The structural responses of substructures that have rigid body modes when separated from the remainder of the structure are further decomposed into displacements that have no rigid body components, and a set of rigid body modes. The structural-response subproblems are linked together through forces determined within a structural-sizing coordination subproblem which also determines the magnitude of any rigid body displacements. Structural-sizing subproblems having constraints local to the substructures are linked together through penalty terms that are determined by a structural-sizing coordination subproblem. All the substructure structural-response subproblems are totally decoupled from each other, as are all the substructure structural-sizing subproblems, thus there are is significant potential for use of parallel solution methods for these subproblems.

14. SUBJECT TERMS
Equilibrium programming, optimization, structural design, structural analysis, nonlinear programming

15. NUMBER OF PAGES
15

16. PRICE CODE
A03

17. SECURITY CLASSIFICATION OF REPORT	18. SECURITY CLASSIFICATION OF THIS PAGE	19. SECURITY CLASSIFICATION OF ABSTRACT	20. LIMITATION OF ABSTRACT
Unclassified	Unclassified		

NASA
Technical
Paper
3404

December 1993

Optical Model Analyses of Galactic Cosmic Ray Fragmentation in Hydrogen Targets

Lawrence W. Townsend

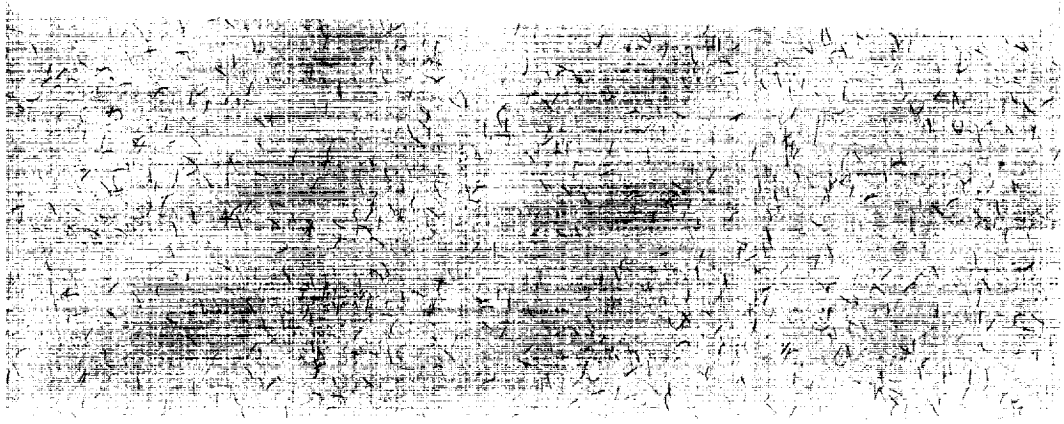

NASA

NASA Technical Paper 3404

1993

Optical Model Analyses of Galactic Cosmic Ray Fragmentation in Hydrogen Targets

Lawrence W. Townsend
Langley Research Center
Hampton, Virginia

NASA
National Aeronautics and Space Administration
Office of Management
Scientific and Technical Information Program

Symbols

A	nuclear mass number
$\binom{A}{B}$	binomial coefficient
$B(e)$	average slope parameter of nucleon-nucleon scattering amplitude, fm^2
$\mathbf{b}$	projectile impact parameter vector, fm
E	energy, GeV or MeV
e	two-nucleon kinetic energy in their center-of-mass frame, GeV
$I(\mathbf{b})$	defined by equation (3)
$I_p(\mathbf{b})$	defined by equation (7)
N	total number of projectile nucleus neutrons
n	number of abraded neutrons
P_{esc}	probability that an abraded nucleon escapes without further interaction
$T(\mathbf{b})$	probability for not removing single nucleon by abrasion
$\mathbf{y}$	two-nucleon relative position vector, fm
Z	total number of projectile-nucleus protons
z	number of abraded protons
$\mathbf{z}_0$	position vector of projectile along beam direction, fm
$\boldsymbol{\xi}_T$	collection of constituent relative coordinates for target, fm
ρ	nuclear single-particle density, fm^{-3}
σ	cross section, fm^2 or mb
λ	mean-free path, fm
Subscripts:	
abr	abraded
exc	prefragment excitation
FSI	frictional spectator interaction
NN	nucleon-nucleon
nuc	nuclear
P	projectile
PF	prefragment
T	target

Abstract

Quantum-mechanical optical model methods for calculating cross sections for the fragmentation of galactic cosmic ray nuclei by hydrogen targets are presented. The fragmentation cross sections are calculated with an abrasion-ablation collision formalism. Elemental and isotopic cross sections are estimated and compared with measured values for neon, sulfur, and calcium ions at incident energies between 400A MeV and 910A MeV. Good agreement between theory and experiment is obtained.

Introduction

The fragmentation of galactic cosmic ray (GCR) nuclei in hydrogen targets is an important physical process in several areas of space radiation physics research. In astrophysics, it is crucial to understanding cosmic ray propagation and source abundances (ref. 1) because interstellar hydrogen is the major type of material encountered by GCR nuclei traveling through the universe. In studies of spacecraft shielding for interplanetary missions (ref. 2), hydrogen has been found to be the most effective GCR shield material per unit mass. In addition, hydrogen is a major constituent of human tissue. Therefore, accurate cross sections are needed for properly estimating GCR radiation exposures to critical body organs (ref. 3).

Previously, cross-section predictions used in these studies have been obtained from semiempirical formulations (refs. 4 to 7). The most commonly used formulation is the one by Silberberg and collaborators (ref. 5). The most accurate formulation appears to be a recent one by Webber and collaborators (ref. 6). None are based upon fundamental physics. All have numerous parameters that are adjusted as necessary to fit existing measurements.

The production of fragments in peripheral, relativistic heavy ion collisions has been the subject of numerous theoretical and experimental investigations for about 2 decades. Many of these investigations were summarized in reviews published during this period (refs. 7 to 10). Early attempts to explain fragmentation used statistical models (refs. 11 and 12). These were followed by a two-step abrasion-ablation model (ref. 13), which was based upon earlier work by Serber in high-energy, inelastic nuclear collisions (ref. 14).

The main shortcoming associated with the use of early abrasion-ablation models for nuclear fragmentation on hydrogen targets is the unrealistically large proton radius needed for the prefragment excitation energy estimate. This radius is dictated by the reliance on excess surface energy of the misshapen liquid drop as the only source of prefragment excitation.

This shortcoming in the model can be rectified by considering an abrasion-ablation frictional-spectator-interaction (FSI) model where the abrasion stage is described by a quantum-mechanical optical model formalism and the ablation stage is modeled with cascade-evaporation techniques. There is no excess surface area energy. Instead, the prefragment excitation energy is assumed to be provided by FSI contributions from the abraded nucleons. This fragmentation model is proposed in this report.

Abrasion-Ablation Models

In an abrasion-ablation model, the projectile nuclei, moving at relativistic speeds, collide with stationary target nuclei. In the abrasion step (particle knockout), those portions of the nuclear volumes that overlap are sheared away by the collision. The remaining projectile piece, called a prefragment, continues its trajectory with essentially its precollision velocity. Because of the dynamics of the abrasion process, the prefragment is highly excited and subsequently decays

by the emission of gamma radiation or nuclear particles. This step is the ablation stage. The resultant isotope is the nuclear fragment whose cross section is measured. The abrasion step is often formulated with methods obtained from quantum scattering theory (refs. 15 and 16) or with classical geometry arguments (refs. 13 and 17). The ablation step is typically modeled with compound nucleus decay (refs. 13 and 18) or combined cascade-evaporation (ref. 19) methods. Other approaches based upon nuclear Weiszäcker-Williams methods (ref. 20) and nucleon-nucleon cascade plus statistical decay models (ref. 21) have also been proposed.

Although abrasion-ablation fragmentation models have been quite successful in predicting fragment production cross sections, their predictive accuracy is hampered by the need to estimate the (unknown) prefragment excitation energy. Various models have been developed for this purpose (refs. 13, 15, 18, and 22). The most widely used excitation energy formalism (ref. 13) treats the fragmenting nucleus as a misshapen liquid drop whose excitation is given by the excess surface energy resulting from the abrasion step. Although this method worked fairly well for nucleus-nucleus fragmentations, its use in nucleus-hydrogen collisions, among other difficulties, required an artificially large proton radius (ref. 13).

When it was recognized that additional excitation energy was required to improve the agreement between theory and experiment for nucleus-nucleus collisions, the concept of FSI energy was introduced (ref. 22). This concept is based upon the assumption that some abraded nucleons are scattered into rather than away from the prefragment, thereby depositing additional excitation energy. This concept significantly improved the agreement between theory and experiment.

Over the past 10 years, we have formulated an optical model abrasion-ablation–FSI description of fragmentation in relativistic nucleus-nucleus collisions that is used to predict fragment production cross sections (refs. 16 and 23 to 42) and momentum distributions of the emitted fragments (refs. 43 through 47). In the present work, this fragmentation model is modified to make it applicable to nucleus-nucleon collisions. As previously discussed, the main shortcoming associated with the use of early abrasion-ablation models for nuclear fragmentation on hydrogen targets is the unrealistically large proton radius needed for the prefragment excitation energy estimate. This radius is dictated by the reliance on excess surface energy of the misshapen liquid drop as the only source of prefragment excitation.

This shortcoming in the model can be rectified by considering the physics of the fragmentation process. For instance, a picture of overlapping nuclear volumes being sheared off may be reasonable for heavier nuclei colliding with each other, but it is not reasonable for a single nucleon striking another nucleus. Instead, a more reasonable physical picture involves individual collisions between the projectile constituents and the target proton. Some struck projectile nucleons exit the fragmenting nucleus without further interaction, and some interact one or more times with the remaining constituents before departing. The remaining nucleus (prefragment), in an excited state because of the energy deposited during the collision, then deexcites by particle- or gamma-emission processes. This picture is easily described by an abrasion-ablation–FSI model where the abrasion stage is described by a quantum-mechanical optical model formalism and the ablation stage is modeled with cascade-evaporation techniques. There is no excess surface area energy. Instead, the prefragment excitation energy is assumed to be provided by FSI contributions from the abraded nucleons. This fragmentation model is proposed in this report.

Theory

In the nucleus-nucleus optical potential formalism (ref. 29), the cross section for producing, by abrasion, a prefragment of charge Z_{PF} and mass A_{PF} is given by

$$\sigma_{\mathrm{abr}}(Z_{\mathrm{PF}}, A_{\mathrm{PF}}) = \binom{N}{n}\binom{Z}{z}\int d^2b[1-T(\mathbf{b})]^{n+z}[T(\mathbf{b})]^{A_{\mathrm{PF}}} \tag{1}$$

where

$$T(\mathbf{b}) = \exp[-A_T\ \sigma_{NN}(e) I(\mathbf{b})] \tag{2}$$

and

$$I(\mathbf{b}) = [2\pi B(e)]^{-3/2} \int dz_0 \int d^3\boldsymbol{\xi}_T \rho_T(\boldsymbol{\xi}_T) \int d^3y \rho_P(\mathbf{b} + \mathbf{z}_0 + \mathbf{y} + \boldsymbol{\xi}_T) \exp[-y^2/2B(e)] \tag{3}$$

The nuclear number densities $\rho_i (i = P \text{ or } T)$ are obtained from the appropriate charge densities by an unfolding procedure (ref. 16). The constituent-averaged nucleon-nucleon cross sections $\sigma_{NN}(e)$ are given in reference 48. Values for the diffractive nucleon-nucleon scattering slope parameter $B(e)$ are obtained from the parameterization in reference 49.

In equation (1) a hypergeometric charge dispersion model is chosen to describe the distribution of abraded nucleons. The model assumes that z out of Z projectile protons and n out of N projectile neutrons are abraded where

$$N + Z = A_P \tag{4}$$

$$A_{\mathrm{PF}} = A_P - n - z \tag{5}$$

and $\begin{pmatrix} A \\ B \end{pmatrix}$ denotes the usual binomial coefficient expression from probability theory.

For nuclear collisions with hydrogen (proton) targets, the appropriate target number density to use is given by the Dirac delta function

$$\rho_T(\boldsymbol{\xi}_T) = \delta(\boldsymbol{\xi}_T) \tag{6}$$

Inserting equation (6) into equation (3) yields

$$I_p(\boldsymbol{b}) = [2\pi B(e)]^{-3/2} \int dz_0 \int d^3y \rho_P(\mathbf{b} + \mathbf{z}_0 + \mathbf{y}) \exp[-y^2/2B(e)] \tag{7}$$

With $A_T = 1$, equation (2) becomes

$$T(\mathbf{b}) = \exp[-\sigma_{NN}(e) I_p(\mathbf{b})] \tag{8}$$

The nucleus-hydrogen abrasion cross sections are calculated with equations (1), (7), and (8).

Prefragment excitation energies are estimated from the FSI energy contribution

$$E_{\mathrm{exc}} = E_{FSI} \tag{9}$$

which is calculated with the model of Rasmussen (ref. 22). With this model, the rate of energy transfer to the prefragment is

$$\frac{dE}{dx} = \frac{E}{4\lambda} \tag{10}$$

where

$$\lambda = \frac{1}{\rho \sigma_{NN}} \quad \left(\sigma_{NN} \approx \frac{300}{E}\right) \tag{11}$$

yields

$$\frac{dE}{dx} = -12.75 \text{ MeV/fm} \tag{12}$$

If a spherical nucleus of uniform density is assumed, the average energy deposited per interaction is

$$\langle E_{FSI} \rangle \approx 10.2A^{1/3} \text{ MeV} \tag{13}$$

Therefore, the abrasion cross section for a prefragment species $(Z_{\text{PF}}, A_{\text{PF}})$ which has undergone q frictional spectator interactions is

$$\sigma_{\text{abr}}(Z_{\text{PF}}, A_{\text{PF}}, q) = \binom{n+z}{q} (1 - P_{\text{esc}})^q (P_{\text{esc}})^{n+z-q} \sigma_{\text{abr}}(Z_{\text{PF}}, A_{\text{PF}}) \tag{14}$$

where $0 \leq q \leq n + z$, and P_{esc} is the probability that an abraded nucleon escapes without undergoing any frictional spectator interactions (ref. 34). In this report, the choice of $P_{\text{esc}} = 0.5$ follows from the original work of Rasmussen (ref. 22). Such a value assumes that the nuclear surface has no curvature, and this value should be reasonably correct for heavy nuclei. For lighter nuclei, the surface can exhibit significant curvature such that the value of P_{esc} can be larger than 0.5. Methods for estimating P_{esc} when nuclear surface curvature is considered have been formulated by Vary and collaborators (ref. 50).

Depending upon the magnitude of its excitation energy, the prefragment will decay by emitting nucleons, composites, and gamma rays. The probability $\alpha_{ij}(q)$ that a prefragment species j, which has undergone q frictional spectator interactions, deexcites to produce a particular final fragment of type i is obtained with the EVA-3 Monte Carlo cascade-evaporation computer code (ref. 19). Therefore, the final hadronic cross section for production of the type i isotope is obtained from

$$\sigma_{\text{nuc}}(Z_i, A_i) = \sum_j \sum_{q=0}^{n+z} \alpha_{ij}(q) \sigma_{\text{abr}}(Z_j, A_j, q) \tag{15}$$

where the summation over j accounts for contributions from different prefragment isotopes j, and the summation over q accounts for the effects of different FSI excitation energies. Finally, the elemental production cross sections are obtained by summing all isotopes of a given element according to

$$\sigma_{\text{nuc}}(Z_i) = \sum_{A_i} \sigma_{\text{nuc}}(Z_i, A_i) \tag{16}$$

Results

Figures 1 and 2 show isotope production cross sections obtained with equation (15) for ^{32}S beams at 400A MeV fragmenting in hydrogen targets. The figures also show recently reported experimental results (ref. 51). For clarity, the experimental error bars are not plotted. The ^{32}S nuclear density used in the calculation was a Woods-Saxon form with skin thickness and half-density radius obtained from reference 48. The agreement between theory and experiment is quite good, especially considering that no arbitrary parameters are in the theory. Quantitatively, a distribution analysis of the cross-section differences between theory and experiment finds that 32 percent agree within the experimental uncertainties, 50 percent agree within a 25-percent difference, nearly 75 percent agree within a 50-percent difference, and over 82 percent agree within a factor of 2.

Elemental production cross-section predictions obtained from equation (16) are displayed in figures 3 to 8 for ^{20}Ne beams at 400A MeV and 910A MeV and for ^{32}S and ^{40}Ca beams at

400A MeV and 800A MeV incident kinetic energies colliding with hydrogen targets. The nuclear densities used in the calculations were Woods-Saxon forms with skin thicknesses and half-density radii again obtained from reference 48. These experimental data were taken from reference 51. Overall, the agreement between theory and experiment is good, although the theory tends to predict values that are slightly larger than the reported measurements.

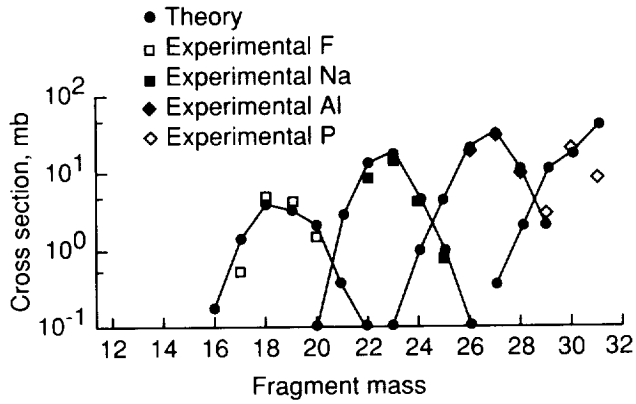

Figure 1. Isotope production cross sections for 400A MeV ^{32}S fragmentation in hydrogen targets for isotopes of P, Al, Na, and F fragments.

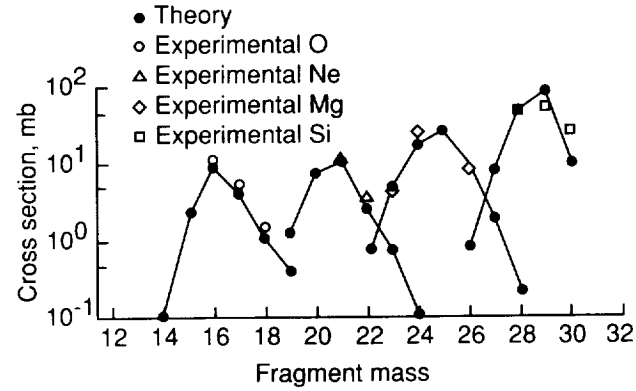

Figure 2. Isotope production cross sections for 400A MeV ^{32}S fragmentation in hydrogen targets for isotopes of Si, Mg, Ne, and O fragments.

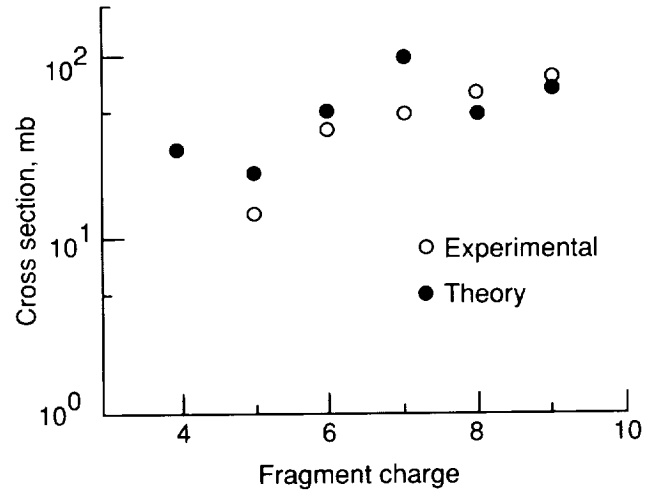

Figure 3. Element production cross sections for 400A MeV ^{20}Ne fragmentation in hydrogen targets.

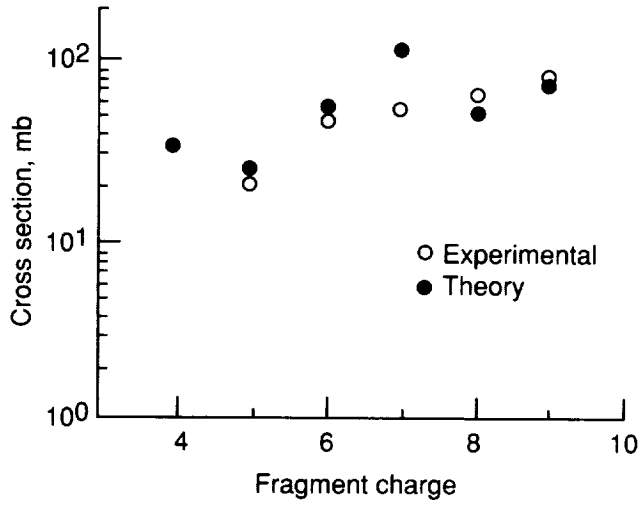

Figure 4. Element production cross sections for 910A MeV ^{20}Ne fragmentation in hydrogen targets.

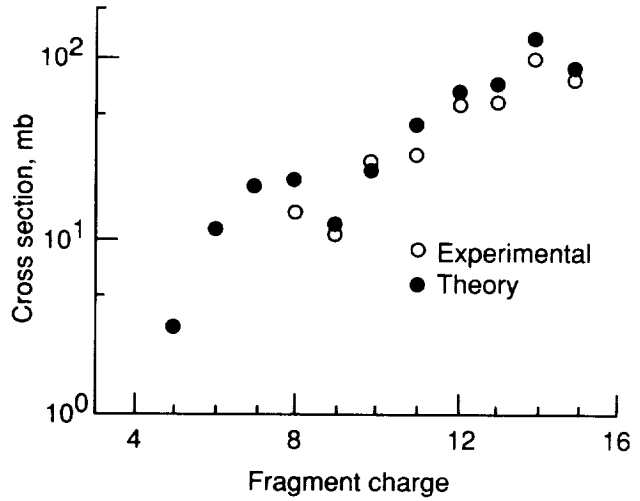

Figure 5. Element production cross sections for 400A MeV ^{32}S fragmentation in hydrogen targets.

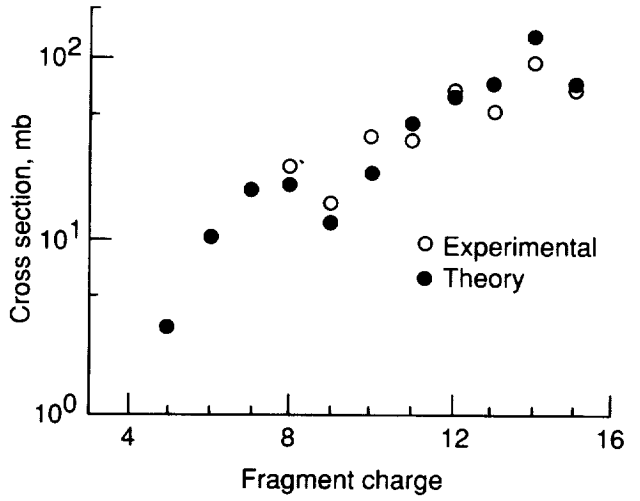

Figure 6. Element production cross sections for 800A MeV ^{32}S fragmentation in hydrogen targets.

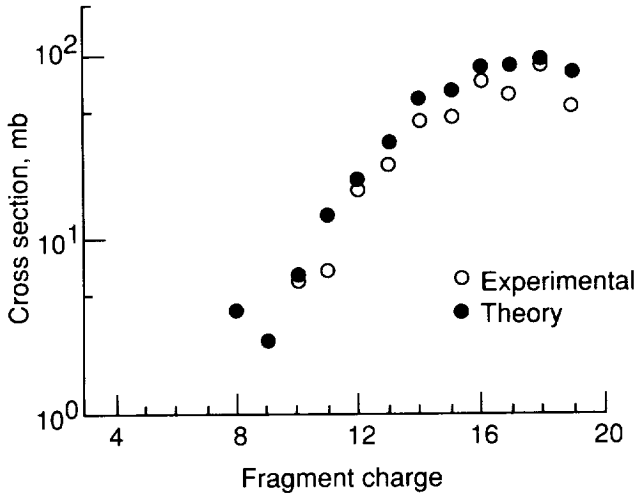

Figure 7. Element production cross sections for 400A MeV ^{40}Ca fragmentation in hydrogen targets.

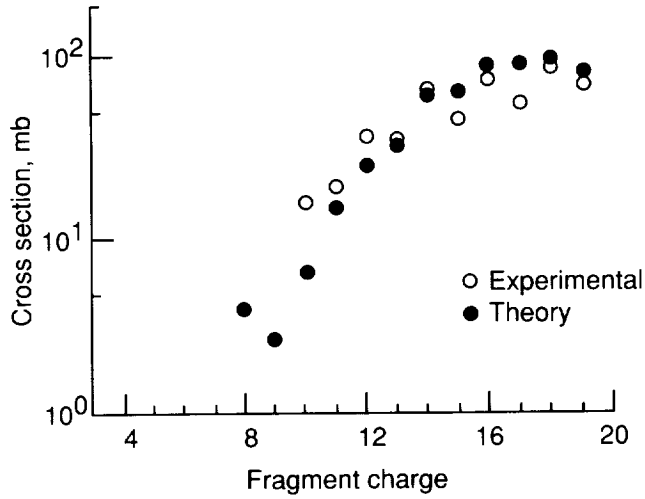

Figure 8. Element production cross sections for 800A MeV ^{40}Ca fragmentation in hydrogen targets.

Concluding Remarks

A simple, yet accurate, optical potential abrasion-ablation fragmentation model has been developed for use in studies of galactic cosmic ray breakup on hydrogen targets. The model has no arbitrarily adjusted parameters. Model predictions have good agreement with recent laboratory measurements of elemental and isotopic production cross sections for the fragmenting of neon, sulfur, and calcium beams on hydrogen targets.

NASA Langley Research Center
Hampton, VA 23681-0001
October 28, 1993

References

1. Wefel, John P.: An Overview of Cosmic-Ray Research—Composition, Acceleration, and Propagation. *Genesis and Propagation of Cosmic Rays*, Maurice M. Shapiro and John P. Wefel, eds., D. Reidel Publ. Co., 1988, pp. 1–40.

2. Townsend, L. W.; and Wilson, J. W.: Interaction of Space Radiation With Matter. IAF/IAA-90-543, Oct. 1990.

3. Wilson, John W.; Townsend, Lawrence W.; Schimmerling, Walter; Khandelwal, Govind S.; Khan, Ferdous; Nealy, John E.; Cucinotta, Francis A.; Simonsen, Lisa C.; Shinn, Judy L.; and Norbury, John W.: *Transport Methods and Interactions for Space Radiations.* NASA RP-1257, 1991.

4. Rudstam, G.: Systematics of Spallation Yields. *Zeitschrift fur Naturforschung*, vol. 21a, no. 7, July 1966, pp. 1027–1041.

5. Silberberg, R.; Tsao, C. H.; and Letaw, John R.: Improvement of Calculations of Cross Sections and Cosmic-Ray Propagation. *Composition and Origin of Cosmic Rays*, Maurice M. Shapiro, ed., D. Reidel Publ. Co., c.1983, pp. 321–336.

6. Webber, W. R.; Kish, J. C.; and Schrier, D. A.: Formula for Calculating Partial Cross Sections for Nuclear Reactions of Nuclei With $E \gtrsim 200$ MeV/Nucleon in Hydrogen Targets. *Phys. Review C*, vol. 41, no. 2, Feb. 1990, pp. 566–571.

7. Townsend, Lawrence W.; Wilson, John W.; Tripathi, Ram K.; Norbury, John W.; Badavi, Francis F.; and Khan, Ferdous: *HZEFRG1: An Energy-Dependent Semiempirical Nuclear Fragmentation Model.* NASA TP-3310, 1993.

8. Goldhaber, Alfred S.; and Heckman, Harry H.: High Energy Interactions of Nuclei. *Annual Review of Nuclear and Particle Science*, vol. 28, J. D. Jackson, Harry E. Gove, and Roy F. Schwitters, eds., Annual Reviews Inc., 1978, pp. 161–205.

9. Hüfner, J.: Heavy Fragments Produced in Proton-Nucleus and Nucleus-Nucleus Collisions at Relativistic Energies. *Phys. Rep.*, vol. 125, no. 4, Aug. 1985, pp. 129–185.

10. Bromley, D. Allan, ed.: *Treatise on Heavy-Ion Science.* Plenum Press.
    Volume 1—Elastic and Quasi-Elastic Phenomena. c.1984.
    Volume 2—Fusion and Quasi-Fusion Phenomena. c.1984.
    Volume 3—Compound System Phenomena. c.1985.
    Volume 4—Extreme Nuclear States. c.1985.
    Volume 5—High-Energy Atomic Physics. c.1985.
    Volume 6—Astrophysics, Chemistry, and Condensed Matter. c.1985.
    Volume 7—Instrumentation and Techniques. c.1985.
    Volume 8—Nuclei Far From Stability. c.1989.

11. Feshbach, H.; and Huang, K.: Fragmentation of Relativistic Heavy Ions. *Phys. Lett.*, vol. 47B, no. 4, Nov. 26, 1973, pp. 300–302.

12. Goldhaber, A. S.: Statistical Models of Fragmentation Processes. *Phys. Lett.*, vol. 53B, no. 4, Dec. 23, 1974, pp. 306–308.

13. Bowman, J. D.; Swiatecki, W. J.; and Tsang, C. F.: *Abrasion and Ablation of Heavy Ions.* LBL-2908, Lawrence Berkeley Lab., Univ. of California, July 1973.

14. Serber, R.: Nuclear Reactions at High Energies. *Phys. Review*, vol. 72, no. 11, Dec. 1, 1947, pp. 1114–1115.

15. Hüfner, J.; Schäfer, K.; and Schürmann, B.: Abrasion-Ablation in Reactions Between Relativistic Heavy Ions. *Phys. Review*, ser. C, vol. 12, no. 6, Dec. 1975, pp. 1888–1898.

16. Townsend, L. W.: Abrasion Cross Sections for ^{20}Ne Projectiles at 2.1 GeV/Nucleon. *Canadian J. Phys.*, vol. 61, no. 1, Jan. 1983, pp. 93–98.

17. Gosset, J.; Gutbrod, H. H.; Meyer, W. G.; Poskanzer, A. M.; Sandoval, A.; Stock, R.; and Westfall, G. D.: Central Collisions of Relativistic Heavy Ions. *Phys. Review C*, vol. 16, no. 2, Aug. 1977, pp. 629–657.

18. Gaimard, J.-J.; and Schmidt, K.-H.: A Reexamination of the Abrasion-Ablation Model for the Description of the Nuclear Fragmentation Reaction. *Nucl. Phys.*, vol. A531, 1991, pp. 709–745.

19. Morrissey, D. J.; Oliveira, L. F.; Rasmussen, J. O.; Seaborg, G. T.; Yariv, Y.; and Fraenkel, Z.: Microscopic and Macroscopic Model Calculations of Relativistic Heavy-Ion Fragmentation Reactions. *Phys. Review Lett.*, vol. 43, no. 16, Oct. 15, 1979, pp. 1139–1142.

20. Feshbach, Herman; and Zabek, Mark: Fragmentation of Relativistic Heavy Ions. *Ann. Phys.*, vol. 107, nos. 1–2, Sept. 6, 1977, pp. 110–125.

21. Harvey, Bernard G.: Beam-Velocity Fragment Yields and Momenta in Nucleus-Nucleus Collisions From 20 MeV/Nucleon to 200 GeV/Nucleon. *Phys. Review C*, vol. 45, no. 4, Apr. 1992, pp. 1748–1756.

22. Oliveira, Luiz F.; Donangelo, Raul; and Rasmussen, John O.: Abrasion-Ablation Calculations of Large Fragment Yields From Relativistic Heavy Ion Reactions. *Phys. Review C*, vol. 19, no. 3, Mar. 1979, pp. 826–833.

23. Townsend, Lawrence W.: *Ablation Effects in Oxygen-Lead Fragmentation at 2.1 GeV/Nucleon.* NASA TM-85704, 1984.

24. Townsend, Lawrence W.; Wilson, John W.; Norbury, John W.; and Bidasaria, Hari B.: *An Abrasion-Ablation Model Description of Galactic Heavy-Ion Fragmentation.* NASA TP-2305, 1984.

25. Norbury, John W.; Townsend, Lawrence W.; and Deutchman, Philip A.: *A T-Matrix Theory of Galactic Heavy Ion Fragmentation.* NASA TP-2363, 1985.

26. Townsend, L. W.; Wilson, J. W.; and Norbury, J. W.: A Simplified Optical Model Description of Heavy Ion Fragmentation. *Canadian J. Phys.*, vol. 63, no. 2, Feb. 1985, pp. 135–138.

27. Townsend, L. W.; and Norbury, J. W.: *Charge-to-Mass Dispersion Methods for Abrasion-Ablation Fragmentation Models.* NASA TM-86340, 1985.

28. Townsend, Lawrence W.; Wilson, John W.; Cucinotta, Francis A.; and Norbury, John W.: *Optical Model Calculations of Heavy-Ion Target Fragmentation.* NASA TM-87692, 1986.

29. Townsend, L. W.; Wilson, J. W.; Cucinotta, F. A.; and Norbury, J. W.: Comparisons of Abrasion Model Differences in Heavy Ion Fragmentation: Optical Versus Geometric Models. *Phys. Review C*, vol. 34, no. 4, Oct. 1986, pp. 1491–1494.

30. Cucinotta, Francis A.; Norbury, John W.; Khandelwal, Govind S.; and Townsend, Lawrence W.: *Doubly Differential Cross Sections for Galactic Heavy-Ion Fragmentation.* NASA TP-2659, 1987.

31. Cucinotta, Francis A.; Khandelwal, Govind S.; Maung, Khin M.; Townsend, Lawrence W.; and Wilson, John W.: *Eikonal Solutions to Optical Model Coupled-Channel Equations.* NASA TP-2830, 1988.

32. Norbury, John W.; and Townsend, Lawrence W.: Single Nucleon Emission in Relativistic Nucleus-Nucleus Reactions. *Phys. Review C*, third ser., vol. 42, no. 4, Oct. 1990, pp. 1775–1777.

33. Cucinotta, Francis A.; Townsend, Lawrence W.; Wilson, John W.; and Khandelwal, Govind S.: *Inclusive Inelastic Scattering of Heavy Ions and Nuclear Correlations.* NASA TP-3026, 1990.

34. Townsend, Lawrence W.; Norbury, John W.; and Khan, Ferdous: Calculations of Hadronic Dissociation of ^{28}Si Projectiles at 14.6A GeV by Nucleon Emission. *Phys. Review C*, third ser., vol. 43, no. 5, May 1991, pp. R2045–R2048.

35. Cucinotta, Francis A.; Townsend, Lawrence W.; Wilson, John W.; and Norbury, John W.: *Corrections to the Participant-Spectator Model of High-Energy Alpha Particle Fragmentation.* NASA TM-4262, 1991.

36. Cucinotta, Francis A.; Townsend, Lawrence W.; and Wilson, John W.: *Target Correlation Effects on Neutron-Nucleus Total, Absorption, and Abrasion Cross Sections.* NASA TM-4314, 1991.

37. Cucinotta, Francis A.; Townsend, Lawrence W.; and Wilson, John W.: Inclusive Inelastic Scattering of Heavy Ions in the Independent Particle Model. *J. Phys. G: Nucl. Particle Phys.*, vol. 18, no. 5, May 1992, pp. 889–901.

38. Cucinotta, Francis A.; Townsend, Lawrence W.; and Wilson, John W.: *Quasi-Elastic Nuclear Scattering at High Energies.* NASA TM-4362, 1992.

39. Cucinotta, Francis A.; Townsend, Lawrence W.; and Wilson, John W.: Production of ^{3}H at Large Momentum in α-^{12}C Collisions at 2A GeV. *Phys. Lett. B*, vol. 282, no. 1, 2, May 21, 1992, pp. 1–6.

40. Cucinotta, Francis A.; Townsend, Lawrence W.; and Wilson, John W.: Multiple-Scattering Effects in Quasielastic α-^{4}He Scattering. *Phys. Review C*, vol. 46, no. 4, Oct. 1992, pp. 1451–1456.

41. Cucinotta, Francis A.; Townsend, Lawrence W.; and Wilson, John W.: *Description of Alpha-Nucleus Interaction Cross Sections for Cosmic Ray Shielding Studies.* NASA TP-3285, 1993.

42. Townsend, Lawrence W.; Khan, Ferdous; and Tripathi, Ram K.: *Optical Model Calculations of 14.6A GeV Silicon Fragmentation Cross Sections.* NASA TM-4461, 1993.

43. Khan, F.; Khandelwal, G. S.; Townsend, L. W.; Wilson, J. W.; and Norbury, J. W.: Optical Model Description of Momentum Transfer in Relativistic Heavy Ion Collisions. *Phys. Review C*, third ser., vol. 43, no. 3, Mar. 1991, pp. 1372–1377.

44. Townsend, L. W.; Wilson, J. W.; Khan, F.; and Khandelwal, G. S.: Momentum Transfer in Relativistic Heavy Ion Charge Exchange Reactions. *Phys. Review C*, third ser., vol. 44, no. 1, July 1991, pp. 540–542.

45. Tripathi, R. K.; Townsend, L. W.; and Khan, F.: Phenomenology of Flow Disappearance in Intermediate-Energy Heavy Ion Collisions. *Phys. Review C*, vol. 47, no. 3, Mar. 1993, pp. R935–R937.

46. Khan, F.; Townsend, L. W.; Tripathi, R. K.; and Cucinotta, F. A.: Universal Characteristics of Transverse Momentum Transfer in Intermediate Energy Heavy Ion Collisions. *Phys. Review C*, vol. 48, no. 2, Aug. 1993, pp. 926–928.

47. Khan, Ferdous; and Townsend, Lawrence W.: Widths of Transverse Momentum Distributions in Intermediate-Energy Heavy Ion Collisions. *Phys. Review C*, vol. 48, no. 2, Aug. 1993, pp. 513–516.

48. Townsend, Lawrence W.; and Wilson, John W.: *Tables of Nuclear Cross Sections for Galactic Cosmic Rays: Absorption Cross Sections*. NASA RP-1134, 1985.

49. Ringia, F. E.; Dobrowolski, T.; Gustafson, H. R.; Jones, L. W.; Longo, M. J.; Parker, E. F.; and Cork, Bruce: Differential Cross Sections for Small-Angle Neutron-Proton and Neutron-Nucleus Elastic Scattering at 4.8 GeV/c. *Phys. Review Lett.*, vol. 28, no. 3, Jan. 17, 1972, pp. 185–188.

50. Benesh, C. J.; Cook, B. C.; and Vary, J. P.: Single Nucleon Removal in Relativistic Nuclear Collisions. *Phys. Review C*, third ser., vol. 40, no. 3, Sept. 1989, pp. 1198–1206.

51. Guzik, J. G.; Albergo, S.; Chen, C. X.; Costa, S.; Crawford, H. J.; Engelage, J.; Ferrando, P.; Flores, I.; Greiner, L.; Jones, F. C.; Knott, C. N.; Ko, S.; Lindstrom, P. J.; Lynen, U.; Mazotta, J.; Miller, J.; Mitchell, J. W.; Mueller, W. F. J.; Romanski, J.; Potenza, R.; Soutoul, A.; Testard, O.; Tull, C. E.; Tuve, C.; Waddington, C. J.; Webber, W. R.; Wefel, J. P.; and Zhang, X.: A Program To Measure New Energetic Particle Nuclear Interaction Cross Sections. COSPAR Paper No. F2.6-M.2.05.

REPORT DOCUMENTATION PAGE

Form Approved
OMB No. 0704-0188

1. AGENCY USE ONLY *(Leave blank)*	2. REPORT DATE	3. REPORT TYPE AND DATES COVERED
	December 1993	Technical Paper

4. TITLE AND SUBTITLE
Optical Model Analyses of Galactic Cosmic Ray Fragmentation in Hydrogen Targets

5. FUNDING NUMBERS
WU 199-45-16-11

6. AUTHOR(S)
Lawrence W. Townsend

7. PERFORMING ORGANIZATION NAME(S) AND ADDRESS(ES)
NASA Langley Research Center
Hampton, VA 23681-0001

8. PERFORMING ORGANIZATION REPORT NUMBER
L-17306

9. SPONSORING/MONITORING AGENCY NAME(S) AND ADDRESS(ES)
National Aeronautics and Space Administration
Washington, DC 20546-0001

10. SPONSORING/MONITORING AGENCY REPORT NUMBER
NASA TP-3404

11. SUPPLEMENTARY NOTES

12a. DISTRIBUTION/AVAILABILITY STATEMENT
Unclassified Unlimited

Subject Category 73

12b. DISTRIBUTION CODE

13. ABSTRACT *(Maximum 200 words)*

Quantum-mechanical optical model methods for calculating cross sections for the fragmentation of galactic cosmic ray nuclei by hydrogen targets are presented. The fragmentation cross sections are calculated with an abrasion-ablation collision formalism. Elemental and isotopic cross sections are estimated and compared with measured values for neon, sulfur, and calcium ions at incident energies between 400A MeV and 910A MeV. Good agreement between theory and experiment is obtained.

14. SUBJECT TERMS
Nuclear reactions; Galactic cosmic ray interactions; Nuclear spallation products; Frictional spectator interactions

15. NUMBER OF PAGES
13

16. PRICE CODE
A03

17. SECURITY CLASSIFICATION OF REPORT	18. SECURITY CLASSIFICATION OF THIS PAGE	19. SECURITY CLASSIFICATION OF ABSTRACT	20. LIMITATION OF ABSTRACT
Unclassified	Unclassified	Unclassified	